THE JOURNAL OF PHYSICAL CHEMISTRY C

pubs.acs.org/JPCC Article

Twist−Bend Nematic Phase from the Landau−de Gennes Perspective

Lech Longa* and Wojciech Tomczyk*

Cite This: J. Phys. Chem. C 2020, 124, 22761−22775

Read Online

ACCESS | Metrics & More | Article Recommendations | Supporting Information

ABSTRACT: Generalized Landau−de Gennes theory is proposed that comprehensively explains currently available experimental data for the heliconical twist−bend nematic (N_{TB}) phase observed in liquid crystalline systems of chemically *achiral* bent-core-like molecules. A bifurcation analysis gives insight into possible structures that the model can predict and guides in the numerical analysis of relative stability of the isotropic (I), uniaxial nematic (N_U), and twist−bend nematic phases. An estimate of constitutive parameters of the model from temperature variation of the nematic order parameter and the Frank elastic constants in the nematic phase enables us to demonstrate quantitative agreement between the calculated and experimentally determined temperature dependence of the pitch and conical angle in N_{TB}. Properties of order parameters also explain a puzzling lack of a half-pitch band in resonant soft X-ray scattering. Other key findings of the model are predictions of I−N_{TB} and N_U−N_{TB} tricritical points and insight into biaxiality of N_{TB}.

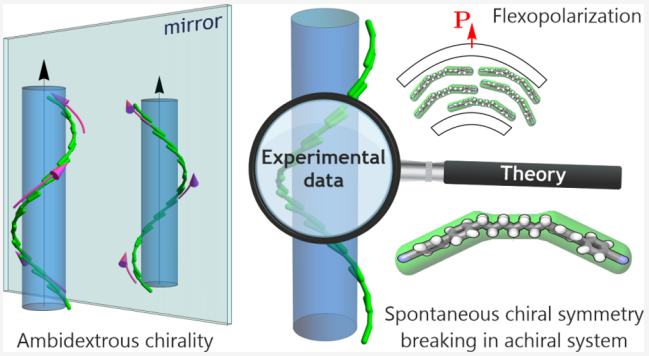

INTRODUCTION

Undoubtedly, the short-pitch heliconical structure formed by an ensemble of achiral bent-core-like mesogens and commonly referred to as the nematic twist−bend is one of the most astonishing liquid crystalline phases. It is the first example in nature of a structure where the mirror symmetry is spontaneously broken without any support from a long-range positional order. The structure itself is a part of an over 130 year-old tradition of liquid crystal science, demonstrating that even a minor change in the molecular chemistry can lead to a new type of liquid crystalline order, which differs in the degree of orientational and translational self-organization, ranging from molecular through nano- to macroscales.[1−3]

The most common of all known liquid crystalline phases is the uniaxial nematic phase (N_U), where anisotropic molecules or molecular aggregates orient, on the average, parallel to each other. Their local, mean orientation at the point $\tilde{\mathbf{r}}$ of coordinates $(\tilde{x},\tilde{y},\tilde{z})$ is described by a single mesoscopic direction $\hat{\mathbf{n}}(\tilde{\mathbf{r}})$ ($|\hat{\mathbf{n}}(\tilde{\mathbf{r}})| = 1$) known as the director. Because of the statistical head-to-tail inversion symmetry of the local molecular arrangement, the director states $\hat{\mathbf{n}}(\tilde{\mathbf{r}})$ and $-\hat{\mathbf{n}}(\tilde{\mathbf{r}})$ are equivalent. With an inversion symmetry and with a rotational symmetry of molecular orientational distribution about $\hat{\mathbf{n}}(\tilde{\mathbf{r}})$, the existence of the director is a basic property that distinguishes the uniaxial nematics from an ordinary isotropic liquid. That is, the N_U phase is a nonpolar 3D liquid with a long-range orientational order characterized by the $\mathcal{D}_{\infty h}$ point group symmetry.

One important consequence of $\hat{\mathbf{n}}(\tilde{\mathbf{r}})$ being indistinguishable from $-\hat{\mathbf{n}}(\tilde{\mathbf{r}})$ is that the primary order parameter of the uniaxial nematics is the second-rank (3×3) traceless and symmetric alignment tensor (the quadrupole moment of the local angular distribution function of the molecules' long axes)

$$\tilde{\mathbf{Q}}_U(\tilde{\mathbf{r}}) = \tilde{S}\left(\hat{\mathbf{n}}(\tilde{\mathbf{r}}) \otimes \hat{\mathbf{n}}(\tilde{\mathbf{r}}) - \frac{1}{3}\mathbf{I}\right) \quad (1)$$

having the components $\tilde{Q}_{U,\alpha\beta}$; $\tilde{S}$ is the scalar order parameter describing the degree of (local) molecular orientational ordering along $\hat{\mathbf{n}}(\tilde{\mathbf{r}})$, and $\mathbf{I}$ denotes the identity matrix.

Beyond conventional uniaxial nematics, further nematic liquid phases, that (by definition) have only short-ranged positional ordering, were recognized. They involve $\mathcal{D}_{2h}$ symmetric biaxial nematics (N_B) for nonchiral materials and cholesteric (N^*) along with blue phases (BP) for chemically chiral mesogens, characterized locally by the $\mathcal{D}_2$ point group symmetry. In order to account for their local orientational order, we need a full, symmetric, and traceless alignment tensor $\tilde{\mathbf{Q}}(\tilde{\mathbf{r}})$ with three different eigenvalues, as opposed to the uniaxial nematic 1, where only two eigenvalues of $\mathbf{Q} \equiv \mathbf{Q}_U$ are different.

Received: June 23, 2020
Revised: August 18, 2020
Published: August 20, 2020

https://dx.doi.org/10.1021/acs.jpcc.0c05711
J. Phys. Chem. C 2020, 124, 22761−22775

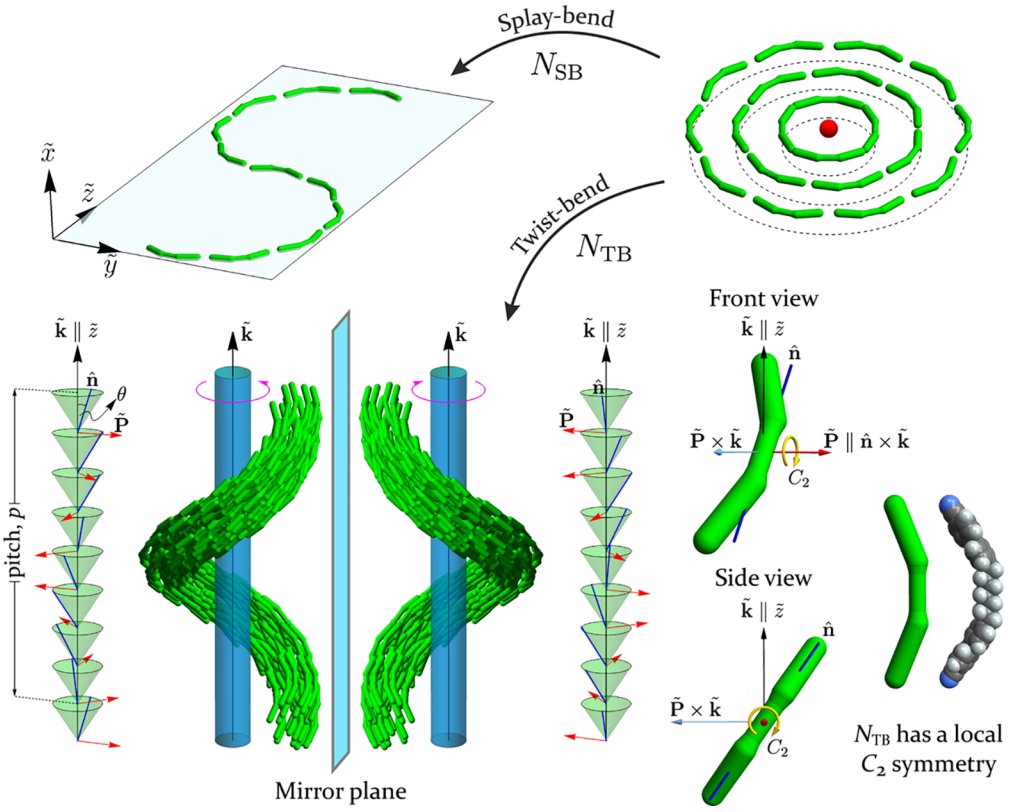

Figure 1. Schematic depiction of modulated nematic phases formed by achiral bent-shaped molecules. Pure bend distortion in 2D leads to the emergence of defects (red sphere). Their appearance can be circumvented by alternating the bend direction periodically or allowing nonzero twist by lifting the bend into the third dimension. These possibilities, respectively, give rise to the two alternative nematic ground states: splay−bend (N_{SB}) and twist−bend (N_{TB}). The twist−bend nematic has been first observed in the phase sequence of the liquid crystal dimer 1″,7″-bis(4-cyanobiphenyl-4′-yl)heptane (CB7CB), where two identical cyanobiphenyl mesogenic groups are linked by a heptane spacer (the CB7CB molecule can be viewed as having three parts: two identical rigid end groups connected by a flexible spacer). Schematic representation of molecular organization in the N_{TB} with right and left handedness (ambidextrous chirality) has been depicted at the bottom of the image. The right/left circular cone of conical angle θ shows the tilt between the director $\hat{\mathbf{n}}$ and the helical symmetry axis, parallel to the wave vector $\tilde{\mathbf{k}}$. The red arrow represents polarization $\tilde{\mathbf{P}}$, where $\tilde{\mathbf{P}} \| \hat{\mathbf{n}} \times \tilde{\mathbf{k}}$. Note that N_{TB} has a local C_2 symmetry with a two-fold symmetry axis around $\tilde{\mathbf{P}}$.

This four-member nematic family is ubiquitous in nature and it has not been expanding for many years.[1] However, very recently, the situation has changed with the important discovery of two fundamentally new nematics: the twist−bend nematic phase (N_{TB})[4−7] and the nematic splay phase (N_S);[8] it seems that these discoveries only mark the beginning of a new, fascinating research direction in soft matter science.[3,9−12]

Without any doubt, the discovered N_{TB} phase is different than 3D liquids known to date because it exhibits a macroscopic chirality while formed from chemically achiral, bent-core-like molecules. A direct manifestation of chirality is an average orientational molecular order that forms a local helix with a pitch spanning from several to over a dozen of nanometers, in the absence of any long-range positional order of molecular centers of mass. N_{TB} is stabilized as a result of (weakly) first-order phase transition from the uniaxial nematic phase or directly from the isotropic phase,[13,14] and therefore, (as already mentioned) its emergence is probably one of the most unusual manifestation of spontaneous mirror symmetry breaking (SMSB) in three-dimensional liquids.

At the theoretical level, the possibility of SMSB in bent-shaped mesogens has been suggested by Meyer already in 1973. He pointed out that bend deformations, which should be favored by bent-shaped molecules, might lead to flexopolarization-induced chiral structures.[15] About 30 years later, Dozov[16] considered the Oseen−Frank (OF) free energy $F_{OF} = \tilde{V}^{-1}\int_{\tilde{V}} f_{OF}\, d^3\tilde{\mathbf{r}}$ of the director field $\hat{\mathbf{n}}(\tilde{\mathbf{r}})$,[17,18] where

$$f_{OF} = \frac{1}{2}[K_{11}(\tilde{\nabla}\cdot\hat{\mathbf{n}})^2 + K_{22}(\hat{\mathbf{n}}\cdot\tilde{\nabla}\times\hat{\mathbf{n}})^2 + K_{33}(\hat{\mathbf{n}}\times\tilde{\nabla}\times\hat{\mathbf{n}})^2] \quad (2)$$

where K_{11}, K_{22}, and K_{33} are splay, twist, and bend elastic constants, respectively. He correlated the possibility of SMSB in nematics with the sign change of the bend elastic constant, K_{33}. In this latter case, in order to guarantee the existence of a stable ground state, some higher order elastic terms had to be added to f_{OF}. Limiting to defect-free structures, Dozov predicted competition between a twist−bend nematic phase, where the director simultaneously twists and bends in space by precessing on the side of a right circular cone, and a planar splay−bend phase with alternating domains of splay and bend, both shown in Figure 1. If we take into account the temperature dependence of the Frank elastic constants, then, the uniaxial nematic phase becomes unstable to the formation of modulated structures at $K_{33} = 0$, which is the critical point of the model. The behavior of the system depends on the relationship between the splay and twist elastic constants. As it turns out, the twist−bend ordering wins if $K_{11} > 2K_{22}$, while the splay−bend phase is more stable if $K_{11} < 2K_{22}$. Assuming that the wave vector $\tilde{\mathbf{k}}$ of N_{TB} stays parallel to the $\hat{\mathbf{z}}$-axis of the laboratory reference frame ($\tilde{\mathbf{k}} = \tilde{k}\hat{\mathbf{z}}$), the

https://dx.doi.org/10.1021/acs.jpcc.0c05711
J. Phys. Chem. C 2020, 124, 22761−22775

symmetry-dictated, gross features of the heliconical N_{TB} structure are essentially accounted for by the uniform director modulation

$$\hat{\mathbf{n}}(\tilde{z}) = \mathcal{R}_{\hat{\mathbf{z}}}(\phi)\hat{\mathbf{n}}(0) = [\cos(\phi)\sin(\theta),\ \sin(\phi)\sin(\theta),\ \cos(\theta)] \quad (3)$$

where $\hat{\mathbf{n}}(0) = [\sin(\theta),0,\cos(\theta)]$ and $\mathcal{R}_{\hat{\mathbf{z}}}(\phi) = \mathcal{R}_{\hat{\mathbf{z}}}(\phi(\tilde{z}))$ is the homogeneous rotation about $\hat{\mathbf{z}}$ through the azimuthal angle $\phi(\tilde{z}) = \pm\tilde{k}\tilde{z} = \pm 2\pi\tilde{z}/p$, where p is the pitch. The $\pm$ sign indicates that both left-handed and right-handed chiral domains should form with the same probability, which is the manifestation of SMSB in the bulk. Note that the molecules in N_{TB} are inclined, on the average, from $\tilde{\mathbf{k}}$ by the conical (tilt) angle θ—the angle between $\hat{\mathbf{n}}$ and the wave vector $\tilde{\mathbf{k}}$ (Figure 1). The symmetry of N_{TB} also implies that the structure must be locally polar with the polarization vector, $\tilde{\mathbf{P}}$, staying perpendicular both to the director and the wave vector

$$\tilde{\mathbf{P}}(\tilde{z}) = \mathcal{R}_{\hat{\mathbf{z}}}(\phi)\tilde{\mathbf{P}}(0) = \tilde{p}_0[\sin(\phi),\ -\cos(\phi),\ 0] \quad (4)$$

Hence, in the nematic twist—bend phase, both $\hat{\mathbf{n}}$ and $\tilde{\mathbf{P}}$ rotate along the helix direction $\tilde{\mathbf{k}}$, giving rise to a phase with constant bend and twist deformation of no mass density modulation (Figure 1).

In 2013, Shamid et al.[19] developed Landau theory for bend flexoelectricity and showed that the results of Dozov are in line with Meyer's idea of flexopolarization-induced N_{TB}. Their theory predicts a continuous $N-N_{TB}$ transition, where the effective bend elastic constant, renormalized by the flexopolarization coupling, changes sign for sufficiently large coupling. The corresponding structure develops a modulated polar order, averaging to zero globally as in eq 4. Dozov's model is also supported by measurements of anomalously small bend elastic constant (compared to the splay and twist elastic constant) in the nematic phase of materials exhibiting N_{TB} (see, *e.g.*, measurements for the CB7CB dimer of Babakhanova et al.[20−22]).

The second most widely used continuum model to characterize orientational properties of nematics is the minimal coupling, SO(3)-symmetric Landau—de Gennes (LdeG) expansion in terms of the local alignment tensor. It allows us not only to account for a fine structure of inhomogeneous nematic phases but also shows important generalizations of the director's description in dealing with orientational degrees of freedom (see, *e.g.*, ref 23). In a series of papers,[11,12,24] coauthored by one of us, we developed an extension of LdeG theory to include flexopolarization couplings. The extended theory predicted that the flexopolarization mechanism can make the N_{TB} phase absolutely stable within the whole family of one-dimensional modulated structures.[11] A qualitatively correct account of experimental observations in N_{TB} (see, *e.g.*, ref 3) was obtained, such as trends in temperature variation of the helical pitch and conical angle and behavior in the external electric field.[25] The theory also predicted weakly first-order phase transitions from the isotropic and nematic to nematic twist—bend phase, again in agreement with experiments.[14,26] Despite this qualitative success of the LdeG modelling, one important theoretical issue still left unsolved is associated with the elastic behavior of the uniaxial nematic phase for materials with stable N_{TB}. A few existing measurements of all three elastic constants in the N_U phase show that $K_{11} \gtrsim 2K_{22}$ ($K_{22} \approx 3-4$ pN), while $K_{33} \approx 0.4$ pN near the transition into N_{TB}.[20] That is, the splay elastic constant is about 20 times larger than the bend elastic constant. On the theoretical side, the LdeG expansion with only two distinct bulk elastic terms cannot explain this anomalously large disparity in the values of K_{11} and K_{33}. Actually, it predicts that they both are equal in the OF limit,[27,28] where the alignment tensor is given by eq 1. Therefore, there are anomalously small bend and splay Frank elastic constants on approaching N_{TB} in the LdeG model with flexopolarization.[12] Although this prediction might suggest dominance of the structures with splay—bend deformations over that of the twist—bend ones, the N_{TB} phase, as already discussed before, can still be found to be more stable than any of one-dimensional periodic structures, including the nematic splay—bend phase.[11] Most probably, this is due to the remarkable (and unique) feature of N_{TB} being uniform everywhere in space that makes the SO(3)-symmetric elastic free-energy density independent of space variables.[11]

Central to quantitative understanding of N_{TB} and related phase transitions is the construction of generalized LdeG theory that releases the $K_{11} = K_{33}$ restriction of the minimal coupling model and accounts for the experimental behavior of the Frank elastic constants in the vicinity of N_U-N_{TB} phase transition. We expect that such a theory will allow for a systematic study of mesoscopic mechanisms that can be responsible for chiral symmetry breaking in nematics. It will also give a new insight into conditions that can potentially lead experimentalists to the discovery of new nematic phases. Although the choice of strategy has already been worked out in the literature,[24,29,30] the main problem lies in a huge number of elastic invariants in the alignment tensor, contributing to the generalized elastic free-energy density of nematics. Here, we show how the problem can be solved in a systematic way if we start from a theory which holds without limitations for arbitrary one-dimensional periodic distortions of the alignment tensor that serve as ground states. These ground states form the most interesting class of structures for it obeys the recently discovered new nematic phases. An additional requirement for generalized LdeG theory is that its *ground state in the absence of flexopolarization* should be that corresponding to a constant tensor field $\tilde{\mathbf{Q}}$. The theory so constructed will then be applied to characterize properties of N_{TB} formed in the class of CB7CB-like dimers and its constitutive parameters will be estimated from experimental data known for the CB7CB dimers in the N_U phase.

THEORETICAL METHODS

Alignment Tensor Representation for Homogeneously Deformed Nematic Phases. In the N_{TB} phase, the director $\hat{\mathbf{n}}$ and the polarization vector $\tilde{\mathbf{P}}$ are given by eqs 3 and 4, while the equivalent alignment tensor order parameter, $\tilde{\mathbf{Q}}_{U,TB}$, is obtained by substituting 3 into 1. Although these models seem to account for gross features of the orientational order observed in N_{TB}, they do not exhaust possible nematic structures that can fill space with twist, bend, and splay. A full spectrum of possibilities is obtained by studying an expansion of the biaxial alignment tensor $\tilde{\mathbf{Q}}$ and the polarization field $\tilde{\mathbf{P}}$ in spin tensor modes of $L = 2$ and $L = 1$, respectively, and in plane waves.[12] Within this huge family of states, an important class of nematic states is represented by uniformly deformed structures (UDSs) where the elastic, SO(3)-symmetric invariants contributing to the elastic free-energy density of nematics[24,30] are constant in space. For such structures, the same tensor and polarization landscape is seen everywhere in space. They are periodic in, at most, one spatial direction, say $\tilde{z}$, and uniformly fill space without defects. In analogy to the conditions 3 and 4 for $\hat{\mathbf{n}}$ and $\tilde{\mathbf{P}}$, they are generated from the tensors $\tilde{\mathbf{Q}}(0)$ and $\tilde{\mathbf{P}}(0)$ for $\tilde{z} = 0$ by

https://dx.doi.org/10.1021/acs.jpcc.0c05711
J. Phys. Chem. C 2020, 124, 22761−22775

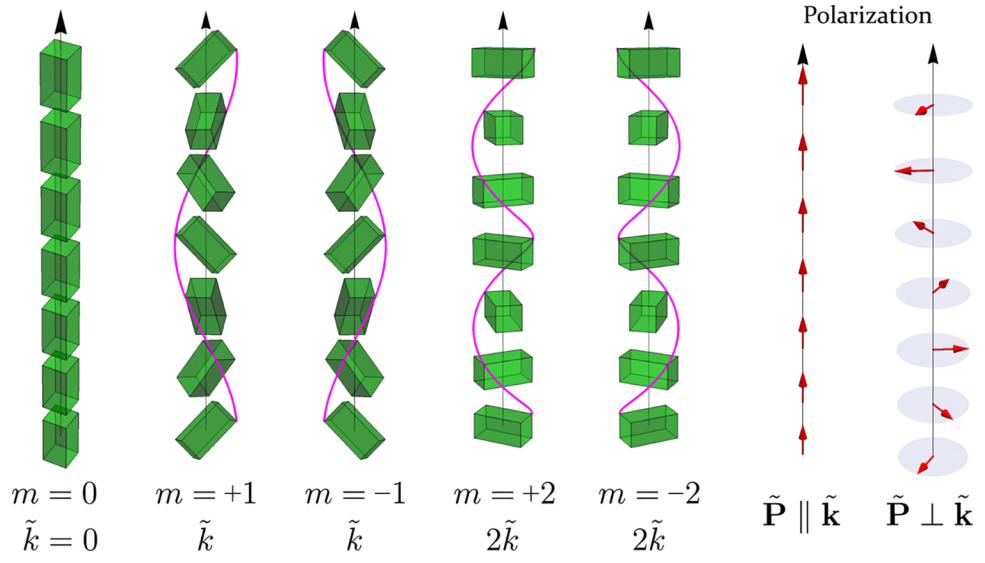

Figure 2. Visualization of helicity modes introduced in eqs 6 and 7: indices $m = 0$, $m = \pm 1$, and $m = \pm 2$ correspond to subscripts 0, ± 1, and ± 2 of $\{\tilde{x}_0, \tilde{v}_0\}$, $\{\tilde{r}_{\pm 1}, \tilde{p}_{\pm 1}\}$, and $\{\tilde{r}_{\pm 2}, \tilde{p}_{\pm 2}\}$, respectively. Change of m into $-m$ corresponds to replacement of $\tilde{\mathbf{k}}$ by $-\tilde{\mathbf{k}}$. Bricks represent the tensor $\tilde{\mathbf{Q}}(\tilde{\mathbf{r}})$ where the eigenvectors of $\tilde{\mathbf{Q}}(\tilde{\mathbf{r}})$ are parallel to their arms, while the absolute values of eigenvalues are their lengths. Red arrows represent the polarization field $\tilde{\mathbf{P}}(\tilde{\mathbf{r}})$.

the previously defined homogeneous rotation $\mathcal{R}_{\hat{\mathbf{z}}}(\pm\tilde{k}\tilde{z}) \equiv \mathcal{R}_{\hat{\mathbf{z}}}(\phi)$.[11,31] More specifically

$$\mathcal{R}_{\hat{\mathbf{z}}}(\pm\tilde{k}\tilde{z})\tilde{\mathbf{Q}}(0) = \tilde{\mathbf{Q}}(\tilde{z})$$
$$\mathcal{R}_{\hat{\mathbf{z}}}(\pm\tilde{k}\tilde{z})\tilde{\mathbf{P}}(0) = \tilde{\mathbf{P}}(\tilde{z}) \tag{5}$$

where $\pm$ labels left- (+) and right-handed (−) heliconical structures. Hence, the most general representations for UDSs that generalize eqs 3 and 4 can be cast in the form (see Figure 2)[11,31]

$$\tilde{\mathbf{Q}}(\tilde{z}) = \frac{\tilde{x}_0}{\sqrt{6}}\begin{bmatrix} -1 & 0 & 0 \\ 0 & -1 & 0 \\ 0 & 0 & 2 \end{bmatrix} + \frac{\tilde{r}_{\pm 1}}{\sqrt{2}}\begin{bmatrix} 0 & 0 & -c_{\pm 1} \\ 0 & 0 & s_{\pm 1} \\ -c_{\pm 1} & s_{\pm 1} & 0 \end{bmatrix} + \frac{\tilde{r}_{\pm 2}}{\sqrt{2}}\begin{bmatrix} c_{\pm 2} & -s_{\pm 2} & 0 \\ -s_{\pm 2} & -c_{\pm 2} & 0 \\ 0 & 0 & 0 \end{bmatrix} \tag{6}$$

$$\tilde{\mathbf{P}}(\tilde{z}) = \tilde{p}_{\pm 1}\begin{bmatrix} -\cos(\pm\tilde{k}\tilde{z} + \phi_{\pm p}) \\ \sin(\pm\tilde{k}\tilde{z} + \phi_{\pm p}) \\ 0 \end{bmatrix} + \tilde{v}_0\begin{bmatrix} 0 \\ 0 \\ 1 \end{bmatrix} \tag{7}$$

where $c_{\pm m} = \cos(\pm m\tilde{k}\tilde{z} + \phi_{\pm m})$ and $s_{\pm m} = \sin(\pm m\tilde{k}\tilde{z} + \phi_{\pm m})$ and nine real parameters $\tilde{x}_0$, $\pm\tilde{k}$, $\tilde{r}_{\pm i} \geq 0$, $\tilde{p}_{\pm 1} \geq 0$, $\tilde{v}_0$, $\phi_{\pm m}$, and $\phi_{\pm p}$ for each of the $\pm$ labels characterize the fine structure of the phases, especially its biaxiality. Indeed, an arbitrary symmetric and traceless tensor field $\tilde{\mathbf{Q}}$ fulfills the inequalities (see discussion in ref 32)

$$-1 \leq w = \frac{\sqrt{6}\,\mathrm{Tr}(\tilde{\mathbf{Q}}^3)}{\mathrm{Tr}(\tilde{\mathbf{Q}}^2)^{3/2}} \leq 1 \tag{8}$$

which are satisfied as equalities for locally prolate ($w = 1$) and oblate ($w = -1$) uniaxial phases. States of nonzero biaxiality are realized for $-1 < w < 1$, with maximal biaxiality corresponding to $w = 0$. In particular, the parameter $w(\tilde{\mathbf{Q}}(\tilde{z}))$ for $\tilde{\mathbf{Q}}(\tilde{z})$ given by eq 6 reads

$$w(\tilde{\mathbf{Q}}(\tilde{z})) = \frac{\frac{3}{2}\tilde{r}_{\pm 1}{}^2(\sqrt{3}\,\tilde{r}_{\pm 2}\cos(2\phi_{\pm 1} - \phi_{\pm 2}) + \tilde{x}_0) - 3\tilde{r}_{\pm 2}{}^2\tilde{x}_0 + \tilde{x}_0{}^3}{(\tilde{r}_{\pm 1}{}^2 + \tilde{r}_{\pm 2}{}^2 + \tilde{x}_0{}^2)^{3/2}} \tag{9}$$

Note that in agreement with definition 5, the parameter $w(\tilde{\mathbf{Q}}(\tilde{z}))$ is position-independent and can take an arbitrary value within the allowed $[-1, 1]$ interval, eq 8. In contrast, for the uniaxial tensor $\tilde{\mathbf{Q}}_{\mathrm{U,TB}}$, corresponding to $\tilde{x}_0 = \frac{\sqrt{6}S}{12}(1 + 3\cos(2\theta))$, $\tilde{r}_{\pm 1} = \frac{\sqrt{2}S}{2}\sin(2\theta)$, and $\tilde{r}_{\pm 2} = \frac{\sqrt{2}S}{2}\sin(\theta)^2$, the parameter $w(\tilde{\mathbf{Q}}_{\mathrm{U,TB}}) = \mathrm{Sign}(S) = \pm 1$ (θ is the conical angle).

We should mention that the fields in eqs 6 and 7 are insensitive to the choice of the origin of the laboratory reference frame, which allows us to eliminate one of the phases $\phi_{\pm i}$ ($i = 1$, 2, p), independently for each of the two states with "+" and "−" subscripts. The coefficients in eqs 6 and 7 are chosen such that the norms squared of the order parameters are sums of squares of the coefficients: $\mathrm{Tr}(\tilde{\mathbf{Q}}^2) = \tilde{x}_0{}^2 + \tilde{r}_{\pm 1}{}^2 + \tilde{r}_{\pm 2}{}^2$ and $\mathrm{Tr}(\tilde{\mathbf{P}}^2) = \tilde{p}_{\pm 1}{}^2 + \tilde{v}_0{}^2$. Together $\tilde{\mathbf{Q}}$ and $\tilde{\mathbf{P}}$ characterize a family of all defect-free uniformly deformed (polar) helical/heliconical nematic phases. They are gathered in Table 1.

Generalized LdeG Expansion for 1D Periodic Nematics. In this section, we introduce a generalized LdeG free-energy expansion in $\tilde{\mathbf{Q}}$ and $\tilde{\mathbf{P}}$, capable of quantitative description of the systems with stable one-dimensional periodic nematics. The most important members of this family are the nematic twist−bend phase[3] and recently discovered nematic splay phase.[8] Our main effort in this and next section will concentrate on the general characterization of LdeG expansion. An example of the UDS with its prominent representative—the $\mathrm{N_{TB}}$ phase—will be studied in great detail. Parameters entering the LdeG expansion will be estimated from experimental data for the CB7CB compound in the uniaxial nematic phase. Then, the properties of the $\mathrm{N_{TB}}$ phase resulting from the so constructed LdeG expansion will be calculated and compared with available experimental data.

https://dx.doi.org/10.1021/acs.jpcc.0c05711
J. Phys. Chem. C 2020, 124, 22761−22775

Table 1. Family of Uniformly Deformed Nematic Structures (UDSs) That Can Be Constructed out of the Fields $\tilde{\mathbf{Q}}$ and $\tilde{\mathbf{P}}$[a]

structure	nonzero amplitudes	abbreviation
Nonpolar Structures		
(a) uniaxial nematic	$\tilde{x}_0$	N_U
(b) biaxial nematic	$\tilde{x}_0, \tilde{r}_1, \tilde{r}_2, \tilde{k} \to 0$	N_B
(c) (ambidextrous) cholesteric	$\tilde{x}_0, \tilde{r}_2, \tilde{k}_{N_C} = 2\tilde{k} \neq 0$	N_C
Locally Polar Structures		
(d) locally polar cholesteric	as in (c), $\tilde{p}_1$	N_{Cl}
(e) nematic twist−bend	$\tilde{x}_0, \tilde{r}_1, \tilde{r}_2, \tilde{p}_1, \tilde{k} \neq 0$	N_{TB}
Globally Polar Structures		
(f) polar (a)−(e)	any of (a)−(e), $\tilde{v}_0$	add subscript "p" to (a)−(e)

[a]Limiting cases of the constant $\tilde{\mathbf{Q}}$ and $\tilde{\mathbf{P}}$ are also included.

We assume that the stabilization of N_{TB} is due to entropic, excluded volume flexopolarization interactions,[33] induced by sterically polar molecular bent cores. The direct interactions between electrostatic dipoles will be disregarded[33] and the long-range polar order will be attributed to the molecular shape polarity. With $\tilde{\mathbf{Q}}$ and $\tilde{\mathbf{P}}$, the general LdeG expansion reads[24,28]

$$\tilde{F} = \frac{1}{\tilde{V}}\int_{\tilde{V}} \tilde{f}_{tot}\, d^3\tilde{\mathbf{r}} = \frac{1}{\tilde{V}}\int_{\tilde{V}} (\tilde{f}_{Qb} + \tilde{f}_{Qel} + \tilde{f}_{P} + \tilde{f}_{QP})d^3\tilde{\mathbf{r}} \tag{10}$$

where $\tilde{\mathbf{r}}$ is the position vector, $\tilde{V}$ is the system's volume, and the free-energy densities $\tilde{f}_{Xx}$ and $\tilde{f}_X$ are constructed out of the fields X. They involve the bulk nematic part $\tilde{f}_{Qb}$, the nematic elastic part $\tilde{f}_{Qel}$, and the parts $\tilde{f}_P$ and $\tilde{f}_{QP}$ responsible for the onset of chirality in the nematic phase. Although the general theory has plenty of constitutive lparameters, part of them, at least for CB7CB, can be estimated from existing experimental data for the N_U and at the I−N_U and N_U−N_{TB} phase transitions. One of the issues we would like to understand is whether the theory so constructed allows us to account for the quantitative properties of the nematic twist−bend phase, below N_U−N_{TB} phase transition.

Bulk Nematic Free Energy. According to phenomenological LdeG theory, the equilibrium bulk properties of nematics can be found from a nonequilibrium free energy, constructed as an SO(3)-symmetric expansion in powers of $\tilde{\mathbf{Q}}$. There are only two types of independent SO(3) invariants that can be constructed out of $\tilde{\mathbf{Q}}$, namely, $\mathrm{Tr}(\tilde{\mathbf{Q}}^2)$ and $\mathrm{Tr}(\tilde{\mathbf{Q}}^3)$. Hence, $\tilde{f}_{Qb}$ is a polynomial in $\mathrm{Tr}(\tilde{\mathbf{Q}}^2)$ and $\mathrm{Tr}(\tilde{\mathbf{Q}}^3)$ with the only restriction on the expansion being that it must be stable against an unlimited growth of $\tilde{\mathbf{Q}}$. The experimental data for $\tilde{S}$ in the nematic phase of CB7CB fit well to a model where the expansion with respect to $\tilde{\mathbf{Q}}$ is taken at least up to sixth-order terms. More specifically, in the absence of electric and magnetic fields, introducing $\tilde{I}_2 = \mathrm{Tr}(\tilde{\mathbf{Q}}^2)$ and $\tilde{I}_3 = \mathrm{Tr}(\tilde{\mathbf{Q}}^3)$, we take for the bulk free-energy density of the isotropic and the nematic phases

$$\begin{aligned}\tilde{f}_{Qb} &= \tilde{f}_{Qb}[\tilde{I}_2, \tilde{I}_3] \\ &= a_Q\tilde{I}_2 - b\tilde{I}_3 + c\tilde{I}_2^{\,2} + d\tilde{I}_2\tilde{I}_3 + e(\tilde{I}_2^{\,3} - 6\tilde{I}_3^{\,2}) + f\tilde{I}_3^{\,2}\end{aligned} \tag{11}$$

A full account of phases and critical and tricritical points that this theory predicts is found in ref 32.

The coefficients of the expansion 11 generally depend on temperature and other thermodynamic variables, but in Landau theory, the explicit temperature dependence is retained only in the bulk part, quadratic in $\tilde{\mathbf{Q}}$. In what follows, as a measure of temperature, we choose the relative temperature distance, Δt, from the nematic−isotropic phase transition, defined through the relation

$$\begin{aligned}a_Q &= a_{0Q}\frac{(T - T^*)}{T_{NI}} = a_{0Q}\left(\frac{T - T_{NI}}{T_{NI}} + \frac{T_{NI} - T^*}{T_{NI}}\right) \\ &= a_{0Q}(\Delta t + \Delta t_{NI})\end{aligned} \tag{12}$$

where $a_{0Q} > 0$, T is the absolute temperature, T_{NI} is the nematic−isotropic transition temperature, T^* is the spinodal for a first-order phase transition from the isotropic phase to the uniaxial nematic phase, $\Delta t = (T - T_{NI})/T_{NI} \leq 0$, and $\Delta t_{NI} = (T_{NI} - T^*)/T_{NI} > 0$ is the reduced temperature distance of nematic−isotropic transition temperature from T^*. Additionally, b, c, d, $e > 0$, and $f > 0$ are the temperature-independent expansion coefficients. The last two conditions for e and f guarantee that $\tilde{f}_{Qb}$ is stable against an unlimited growth of $\tilde{\mathbf{Q}}$.[32] The expansion, eq 11, generally accounts for the isotropic, uniaxial nematic, and biaxial nematic phases.[32,34]

We should mention that the fourth-order expansion, where $c > 0$ and $d = e = f = 0$, predicts that the N_{TB} phase can be absolutely stable within the family of one-dimensional modulated structures,[11] but the theory does not give a quantitative agreement with the data for $\tilde{S}$ in the nematic phase of CB7CB unless an unphysically large value of Δt_{NI} is taken (Figure S1).

Elastic Free Energy. A spatial deformation of the alignment tensor $\tilde{\mathbf{Q}}$ in the nematic phase is measured by the elastic free-energy density $\tilde{f}_{Qel}$ of the Landau free energy expansion 10. For the description of elastic properties of nematic liquid crystals, $\tilde{f}_{Qel}$ usually is expanded into powers of $\tilde{\mathbf{Q}}$ and its first derivatives $\partial\tilde{\mathbf{Q}} \equiv \partial\tilde{Q}_{ij}/\partial\tilde{x}_k = \tilde{Q}_{ij,k}$, where only quadratic terms in derivatives of the order parameter field are retained, in line with similar expansion for the director field, eq 2.

This standard, the so-called minimal-coupling LdeG expansion for $\tilde{f}_{Qel}$, comprises only two bulk elastic terms: $[L_1^{(2)}] = \tilde{Q}_{\alpha\beta,\gamma}\tilde{Q}_{\alpha\beta,\gamma}$ and $[L_2^{(2)}] = \tilde{Q}_{\alpha\beta,\beta}\tilde{Q}_{\alpha\gamma,\gamma}$. Although again the theory, eq 10, with $\tilde{f}_{Qel}$ containing only these two elastic terms accounts for absolutely stable N_{TB} among one-dimensional modulated structures,[11] it is not sufficiently general to quantitatively reproduce, for example, elastic properties of bent-core systems in the parent nematic phase for it implies equality of splay and bend Frank elastic constants, which so far is not an experimentally supported scenario with stable N_{TB}. Thus, we need to include higher order elastic terms in LdeG theory to account for the experimentally observed elastic behavior of bent-core mesogens. A general form of the LdeG elastic free-energy density has been studied by Longa et al. in a series of papers.[24,28,30] As it turns out, the most important are third-order invariants of the form $\tilde{\mathbf{Q}}\partial\tilde{\mathbf{Q}}\partial\tilde{\mathbf{Q}}$, given explicitly in the Supporting Information, because they are the lowest order terms removing splay−bend degeneracy of second-order theory.[28] However, with quadratic and cubic terms alone, the elastic free energy $\tilde{f}_{Qel}$ is unbounded from below and hence cannot represent a correct theory of nematics. To assure that the nematic ground state is stable against an unlimited growth of $\tilde{Q}_{\alpha\beta}$ and $\tilde{Q}_{\alpha\beta,\gamma}$, we need to

https://dx.doi.org/10.1021/acs.jpcc.0c05711
J. Phys. Chem. C 2020, 124, 22761−22775

add some fourth-order invariants.[28] In total, there are 22 deformation modes $[L_i^{(n)}]$ of $\tilde{\mathbf{Q}}$ up to the order $\tilde{\mathbf{Q}}\,\tilde{\mathbf{Q}}\,\partial\tilde{\mathbf{Q}}\,\partial\tilde{\mathbf{Q}}$ (see the Supporting Information for details). The next step is to single out the relevant elastic terms $[L_i^{(n)}]$ that should enter the expansion $\tilde{f}_{\mathrm{Qel}}$. A considerable reduction in the number of independent terms is obtained if we limit ourselves to a class of ground states represented by one-dimensional periodic structures $\tilde{\mathbf{Q}}(\tilde{z}+\tilde{p}) = \tilde{\mathbf{Q}}(\tilde{z})$.[11,35] Then, the only relevant linearly independent $[L]$-terms (nonvanishing for uniaxial $\tilde{\mathbf{Q}}$) are

- $\partial\tilde{\mathbf{Q}}\,\partial\tilde{\mathbf{Q}}$ terms: $[L_1^{(2)}]$, and $[L_2^{(2)}]$
- $\tilde{\mathbf{Q}}\,\partial\tilde{\mathbf{Q}}\,\partial\tilde{\mathbf{Q}}$ terms: $[L_2^{(3)}]$, $[L_3^{(3)}]$, and $[L_4^{(3)}]$
- $\tilde{\mathbf{Q}}\tilde{\mathbf{Q}}\,\partial\tilde{\mathbf{Q}}\,\partial\tilde{\mathbf{Q}}$ terms: $[L_2^{(4)}]$, $[L_3^{(4)}]$, $[L_5^{(4)}]$, $[L_6^{(4)}]$, $[L_7^{(4)}]$, $[L_{10}^{(4)}]$, and $[L_{11}^{(4)}]$.

As mentioned before, the most important are third-order terms $\tilde{\mathbf{Q}}\,\partial\tilde{\mathbf{Q}}\,\partial\tilde{\mathbf{Q}}$ linear in $\tilde{\mathbf{Q}}$ and quadratic in $\partial\tilde{\mathbf{Q}}$ because they remove splay−bend degeneracy.[28] Hence, in what follows, we will keep three third-order terms and add three stabilizing terms of the order $\tilde{\mathbf{Q}}\tilde{\mathbf{Q}}\,\partial\tilde{\mathbf{Q}}\,\partial\tilde{\mathbf{Q}}$. More specifically, for the elastic free energy $\tilde{f}_{\mathrm{Qel}}$, we take a sum of quadratic terms in deformations of the form

$$\begin{aligned}\tilde{f}_{\mathrm{Qel}} &= L_1^{(2)}\tilde{Q}_{\alpha\beta,\gamma}\tilde{Q}_{\alpha\beta,\gamma} + L_2^{(2)}\tilde{Q}_{\alpha\beta,\beta}\tilde{Q}_{\alpha\gamma,\gamma} \\ &\quad + L_{14}^{(4)}(\lambda_2\tilde{Q}_{\mu\nu,\nu} + \tilde{Q}_{\alpha\beta}\tilde{Q}_{\alpha\mu,\beta})^2 \\ &\quad + L_6^{(4)}(\lambda_3\tilde{Q}_{\beta\nu,\nu} + \tilde{Q}_{\alpha\beta}\tilde{Q}_{\alpha\mu,\mu})^2 \\ &\quad + L_7^{(4)}(\lambda_4\tilde{Q}_{\beta\mu,\nu} + \tilde{Q}_{\alpha\beta}\tilde{Q}_{\alpha\mu,\nu})^2 \end{aligned} \tag{13}$$

$$\begin{aligned}&= (L_1^{(2)} + \lambda_4{}^2L_7^{(4)})[L_1^{(2)}] + (L_2^{(2)} + \lambda_2{}^2L_{14}^{(4)} + \lambda_3{}^2L_6^{(4)})[L_2^{(2)}] \\ &\quad + L_2^{(3)}[L_2^{(3)}] + L_{14}^{(4)}[L_{14}^{(4)}] + L_3^{(3)}[L_3^{(3)}] \\ &\quad + L_6^{(4)}[L_6^{(4)}] + L_4^{(3)}[L_4^{(3)}] + L_7^{(4)}[L_7^{(4)}] \end{aligned} \tag{14}$$

where the coefficients, $L_i^{(n)}$, denote temperature−independent elastic constants that couple with the invariant $[L_i^{(n)}]$ and $\lambda_2 = L_2^{(3)}/(2L_{14}^{(4)})$, $\lambda_3 = L_3^{(3)}/(2L_6^{(4)})$, and $\lambda_4 = L_4^{(3)}/(2L_7^{(4)})$. Use of the $[L_{14}^{(4)}]$ invariant, which is a linear combination of the invariants $\tilde{\mathbf{Q}}\tilde{\mathbf{Q}}\,\partial\tilde{\mathbf{Q}}\,\partial\tilde{\mathbf{Q}}$, allows us to write the stability criteria for $\tilde{f}_{\mathrm{Qel}}$ in a simple form (see the Supporting Information). Indeed, the elastic free-energy density $\tilde{f}_{\mathrm{Qel}}$ is a sum of positive definite terms if

$$\begin{aligned} &L_1^{(2)} > 0, \qquad L_1^{(2)} + \frac{2}{3}L_2^{(2)} > 0 \\ &L_6^{(4)} > 0 \vee L_6^{(4)} = 0 \wedge L_3^{(3)} = 0 \\ &L_7^{(4)} > 0 \vee L_7^{(4)} = 0 \wedge L_4^{(3)} = 0 \\ &L_{14}^{(4)} > 0 \vee L_{14}^{(4)} = 0 \wedge L_2^{(3)} = 0 \end{aligned} \tag{15}$$

The conditions 15 are sufficient ones for $\tilde{f}_{\mathrm{Qel}}$ to be positive definite ($\tilde{f}_{\mathrm{Qel}} \geq 0$). For smooth tensor fields $\tilde{\mathbf{Q}}$, the ground state of $\tilde{f}_{\mathrm{Qel}}$ ($\tilde{f}_{\mathrm{Qel}} = 0$) corresponds to a constant, position-independent $\tilde{\mathbf{Q}}$, which represents an unperturbed isotropic, uniaxial, or biaxial nematic state. As we show later in the text, the elastic constants $L_m^{(n)}$ entering expansion 14 can all be estimated from the data for Frank elastic constants in the uniaxial nematic phase. To conclude, the free energy 14 is a thermodynamically stable expansion of the LdeG free energy in the local alignment tensor, complete up to third order for deformations realized in one spatial direction and nonvanishing in the uniaxial limit for $\tilde{\mathbf{Q}}$.

The elastic free energy 14 can still be written in a simpler form by further selecting terms that are relevant for the UDS. Indeed, substitution of eq 6 into expansion 14 induces extra relations between cubic and quartic elastic invariants, namely

$$[L_2^{(3)}] = -2[L_3^{(3)}], \qquad [L_{14}^{(4)}] = 4[L_6^{(4)}] \tag{16}$$

Thus, in seeking for relative stability of the UDS, two elastic terms in 14 are still redundant. This redundancy becomes especially transparent in the parameterization where the elastic constants $L_2^{(3)}$, $L_3^{(3)}$, $L_6^{(4)}$, and $L_{14}^{(4)}$ are replaced by appropriate linear combinations of $L_7^{(3)}$, $L_8^{(3)}$, $L_{15}^{(4)}$, and $L_{16}^{(4)}$. They are given by

$$\begin{aligned} &L_2^{(3)} = L_8^{(3)} - L_7^{(3)}, \qquad L_3^{(3)} = 2(L_8^{(3)} + L_7^{(3)}) \\ &L_6^{(4)} = 4(L_{15}^{(4)} - L_{16}^{(4)}), \qquad L_{14}^{(4)} = L_{15}^{(4)} + L_{16}^{(4)} \end{aligned} \tag{17}$$

where, in addition, the inequality $L_{15}^{(4)} > |L_{16}^{(4)}|$ is required to fulfill stability conditions 15. Substitution of 17 into 14 now yields

$$\begin{aligned}\tilde{f}_{\mathrm{Qel}} &= (L_1^{(2)} + \lambda_4{}^2L_7^{(4)})[L_1^{(2)}] + (L_2^{(2)} + \lambda_2{}^2L_{14}^{(4)} \\ &\quad + \lambda_3{}^2L_6^{(4)})[L_2^{(2)}] + L_7^{(3)}[L_7^{(3)}] + L_{15}^{(4)}[L_{15}^{(4)}] \\ &\quad + L_8^{(3)}[L_8^{(3)}] + L_{16}^{(4)}[L_{16}^{(4)}] + L_4^{(3)}[L_4^{(3)}] + L_7^{(4)}[L_7^{(4)}] \end{aligned} \tag{18}$$

where

$$\begin{aligned} &[L_7^{(3)}] = 2[L_3^{(3)}] - [L_2^{(3)}] \\ &[L_8^{(3)}] = 2[L_3^{(3)}] + [L_2^{(3)}] \\ &[L_{15}^{(4)}] = [L_{14}^{(4)}] + 4[L_6^{(4)}] \\ &[L_{16}^{(4)}] = [L_{14}^{(4)}] - 4[L_6^{(4)}] \end{aligned} \tag{19}$$

where $[L_8^{(3)}]$ and $[L_{16}^{(4)}]$ terms vanish for the UDS, given by eq 6.

Coupling with Steric Polarization. According to the current understanding of the formation of the stable twist−bend nematic phase, its orientational order, being similar to that of smectic C^*,[1] should be accompanied with a long-range polar order of molecular bent cores.[36−40] As already pointed out, the other direct molecular interactions, such as between electrostatic dipoles, are probably less relevant for the thermal stability of this phase. Up to the leading order in $\tilde{\mathbf{P}}$, at least five extra terms must be included in $\tilde{f}_{\mathrm{P}}$ and $\tilde{f}_{\mathrm{QP}}$, eq 10. They read[11,12,28]

$$\tilde{f}_{\mathrm{P}} = a_{\mathrm{P}}\tilde{\mathbf{P}}^2 + A_4(\tilde{\mathbf{P}}^2)^2 + b_{\mathrm{P}}(\tilde{\nabla}\otimes\tilde{\mathbf{P}})^2 \tag{20}$$

$$\tilde{f}_{\mathrm{QP}} = -\varepsilon_{\mathrm{P}}\tilde{\mathbf{P}}\cdot(\tilde{\nabla}\cdot\tilde{\mathbf{Q}}) - \Lambda_{\mathrm{QP}}\tilde{P}_\alpha\tilde{Q}_{\alpha\beta}\tilde{P}_\beta \tag{21}$$

Here, $a_{\mathrm{P}} = a_{0\mathrm{P}}((T - T_{\mathrm{P}})/T_{\mathrm{NI}}) = a_{0\mathrm{P}}(\Delta t + \Delta t_{\mathrm{NI,P}})$, where $\Delta t_{\mathrm{NI,P}} = (T_{\mathrm{NI}} - T_{\mathrm{P}})/T_{\mathrm{NI}} > 0$, $A_4 > 0$, $b_{\mathrm{P}} > 0$, ε_{P}, and Λ_{QP} are further temperature-independent constitutive parameters of the model. Again, limitations for A_4 and b_{P} stem from stability requirement of a ground state against unlimited fluctuations of $\tilde{\mathbf{P}}(\tilde{\mathbf{r}})$. The ε_{P}-term represents lowest order flexopolarization contribution, while the Λ_{QP}-term is the direct coupling between the polarization field and the alignment tensor. The presently existing experimental data seem to be in line with this minimal coupling expansion for the (flexo)polarization part of the free energy.[11,12] A full structure of (flexo)polarization theory, along with some of its general consequences, can be found in ref 24.

https://dx.doi.org/10.1021/acs.jpcc.0c05711
J. Phys. Chem. C 2020, 124, 22761−22775

Reduced Form of Generalized LdeG Expansion. For practical calculations, it is useful to reduce the number of model parameters by rewriting eq 10 in terms of reduced (dimensionless) quantities. It reveals the redundancy of four parameters in the expressions 11, 14, 20, and 21 and allows to set them to one from the start.[12,24,28,29] This reduction is a direct consequence of the freedom to choose a scale for the free energy, $\tilde{F} = \Lambda_F F$, for the fields $\tilde{\mathbf{Q}} = \Lambda_Q \mathbf{Q}$ and $\tilde{\mathbf{P}} = \Lambda_P \mathbf{P}$, for the position vector $\tilde{\mathbf{r}} = \Lambda_r \mathbf{r}$, where Λ_i are nonzero scaling parameters. Taking this freedom into account, we introduce the reduced quantities F (f_{tot}), $\mathbf{Q}$ (equivalently S, x_0, r_1, and r_2), $\mathbf{P}$ (equivalently p_1 and v_0), $\mathbf{r}$, $\mathbf{k}$, t_Q, $\rho_{2,2} - \rho_{4,16}$, t_P, a_d, e_P, λ, c_b, d_b, and e_b with the help of the equations

$$\tilde{F} = \frac{b^2}{f}F \quad \left(\tilde{f}_{tot} = \frac{b^2}{f}f_{tot}\right), \qquad \tilde{\mathbf{r}} = \frac{\sqrt[6]{f}\sqrt{L_1^{(2)}}}{b^{2/3}}\mathbf{r}, \qquad \tilde{\mathbf{Q}} = \sqrt[3]{\frac{b}{f}}\mathbf{Q}$$

$$\tilde{\mathbf{P}} = \sqrt[3]{\frac{b}{f}}\sqrt{\frac{L_1^{(2)}}{b_P}}\mathbf{P}, \qquad a_Q = \sqrt[3]{\frac{b^4}{f}}t_Q, \qquad a_P = \frac{b^{4/3}b_P t_P}{\sqrt[3]{f}L_1^{(2)}}$$

$$L_2^{(2)} = L_1^{(2)}\rho_{2,2}, \qquad L_i^{(3)} = \sqrt[3]{\frac{f}{b}}L_1^{(2)}\rho_{3,i}, \qquad L_i^{(4)} = \sqrt[3]{\left(\frac{f}{b}\right)^2}L_1^{(2)}\rho_{4,i}$$

$$\lambda_i = L_1^{(2)}l_i, \qquad l_2 = \frac{\rho_{3,2}}{2\rho_{4,14}}, \qquad l_3 = \frac{\rho_{3,3}}{2\rho_{4,6}}, \qquad l_4 = \frac{\rho_{3,4}}{2\rho_{4,7}}$$

$$A_4 = \frac{\sqrt[3]{b^2 f}a_d b_P^2}{(L_1^{(2)})^2}, \qquad \varepsilon_P = \frac{b^{2/3}\sqrt{b_P}e_P}{\sqrt[6]{f}}, \qquad \Lambda_{QP} = \frac{bb_P}{L_1^{(2)}}\lambda$$

$$c = \sqrt[3]{b^2 f}c_b, \qquad d = \sqrt[3]{b^2 f^2}\,d_b, \qquad \tilde{\mathbf{k}} = \frac{b^{2/3}}{\sqrt[6]{f}\sqrt{L_1^{(2)}}}\mathbf{k} \tag{22}$$

The remaining quantities (S, x_0, r_1, and r_2) and (p_1 and v_0) are connected with their tilted counterparts by the same relations as $\mathbf{Q}$ with $\tilde{\mathbf{Q}}$ and $\mathbf{P}$ with $\tilde{\mathbf{P}}$, respectively. In addition, the definitions 19 now become reduced to

$$\rho_{3,2} = \rho_{3,8} - \rho_{3,7}, \qquad \rho_{3,3} = 2(\rho_{3,7} + \rho_{3,8})$$
$$\rho_{4,6} = 4(\rho_{4,15} - \rho_{4,16}), \qquad \rho_{4,14} = \rho_{4,15} + \rho_{4,16} \tag{23}$$

Consequently, the generalized LdeG free-energy expansion in terms of reduced variables $\mathbf{Q}$ and $\mathbf{P}$ reads

$$F = \frac{1}{V}\int_V f_{tot}\, d^3\mathbf{r} = \frac{1}{V}\int_V (f_{Qb} + f_{Qel} + f_P + f_{QP})d^3\mathbf{r} \tag{24}$$

where

$$f_{Qb} = f_{Qb}[I_2, I_3] = t_Q I_2 - I_3 + c_b I_2^2 + d_b I_2 I_3 + e_b(I_2^3 - 6I_3^2) + I_3^2 \tag{25}$$

$$\begin{aligned} f_{Qel} = {} & (1 + \rho_{4,7}l_4^2)Q_{\alpha\beta,\gamma}Q_{\alpha\beta,\gamma} \\ & + (\rho_{2,2} + \rho_{4,14}l_2^2 + \rho_{4,6}l_3^2)Q_{\alpha\beta,\beta}Q_{\alpha\gamma,\gamma} \\ & + (\rho_{3,8} - \rho_{3,7})Q_{\alpha\beta}Q_{\alpha\mu,\beta}Q_{\mu\nu,\nu} \\ & + 2(\rho_{3,8} + \rho_{3,7})Q_{\alpha\beta}Q_{\alpha\mu,\mu}Q_{\beta\nu,\nu} \\ & + \rho_{3,4}Q_{\alpha\beta}Q_{\alpha\mu,\nu}Q_{\beta\mu,\nu} + \rho_{4,7}Q_{\alpha\beta}Q_{\gamma\beta}Q_{\alpha\mu,\nu}Q_{\gamma\mu,\nu} \\ & + 4(\rho_{4,15} - \rho_{4,16})Q_{\alpha\beta}Q_{\gamma\beta}Q_{\alpha\mu,\mu}Q_{\gamma\nu,\nu} \\ & + (\rho_{4,15} + \rho_{4,16})Q_{\alpha\beta}Q_{\gamma\delta}Q_{\alpha\mu,\beta}Q_{\gamma\mu,\delta} \end{aligned} \tag{26}$$

$$f_P = t_P\mathbf{P}^2 + a_d(\mathbf{P}^2)^2 + (\nabla \otimes \mathbf{P})^2 \tag{27}$$

$$f_{QP} = -e_P\mathbf{P}\cdot(\nabla\cdot Q) - \lambda P_\alpha Q_{\alpha\beta}P_\beta \tag{28}$$

where $I_2 = \mathrm{Tr}(\mathbf{Q}^2)$ and $I_3 = \mathrm{Tr}(\mathbf{Q}^3)$. In this parameterization, terms proportional to $\rho_{3,8}$ and $\rho_{4,16}$ vanish for the UDS.

The expansions 24 −28 are our LdeG theory of modulated nematics. If we limit ourselves to a family of periodic structures with periodicity being developed in one spatial direction, the nonzero cubic and quartic couplings $\rho_{3,4}$, $\rho_{3,7}$, $\rho_{4,7}$, and $\rho_{4,15}$ should admit the UDS as global minimizers. The remaining two couplings $\rho_{3,8}$ and $\rho_{4,16}$ are solely responsible for one-dimensional, *nonuniform* periodic distortions, which makes the corresponding elastic terms vanish for the UDS. This means that depending on the choice of $\rho_{3,8}$ and $\rho_{4,16}$, we should be able to eliminate inhomogeneously deformed one-dimensional periodic structures from the ground states of LdeG, leaving only the UDS. In the remaining part of this paper, we are going to concentrate exclusively on this simpler case.

Bifurcation Scenarios for Uniformly Deformed Structures. Here, we limit ourselves to the UDS given in Table 1 and determine bifurcation conditions for various symmetry breaking transitions. Clearly, the isotropic-uniaxial nematic bifurcation temperature is given by T^* 12, which represents spinodal, while the I−N_U phase transition takes place at T_{NI}, slightly above T^*. Likewise, T_P entering a_P, eq 20, is transition temperature for a hypothetical phase transition from the isotropic to ferroelectric phase ($\mathbf{P} \neq 0$), in the absence of the nematic order ($\mathbf{Q} = 0$). Both T^* and T_P are examples of bifurcation temperatures from the less-ordered phase (isotropic) to the more ordered one (nematic, ferroelectric). There are further bifurcations possible for the UDSs. Below, we give bifurcation conditions for all possible phase transitions between UDSs given in Table 1. The procedure is found in ref 12 and we only briefly sketch it below. For given material parameters, the equilibrium amplitudes, $y_i \in \{r_1, r_2, p_1, x_0, v_0\}$, are found from the minimization of the free energy F, eq 24, calculated for the UDSs (explicit formula for F is listed in the Supporting Information). They are solutions of a system of polynomial equations $\psi_i(t_Q, t_P, \{y_\alpha\}) \equiv \partial F/\partial y_i = 0$. In order to employ a bifurcation analysis to $\{\psi_\alpha\}$, we expand y_i, t_Q, and t_P in an arbitrary parameter ε

$$y_i = y_{i,0} + \varepsilon y_{i,1} + \varepsilon^2 y_{i,2} + \ldots$$
$$t_m = t_{m,0} + \varepsilon t_{m,1} + \varepsilon^2 t_{m,2} + \ldots \qquad m = Q, P \tag{29}$$

where nonvanishing $y_{i,0}$ defines the reference, higher symmetric phase. For example, if the reference state is the N_U phase, only $y_{4,0} \equiv x_{0,0}$ is nonzero in eq 29. By substituting eq 29 into $\{\psi_\alpha = 0\}$ and letting equations of the same order in ε vanish, we find equations for $y_{i,\alpha}$ and t_m, ($m = Q, P$). The leading terms, proportional to ε^0, are equations describing the high-symmetric reference state. Terms of the order ε^1 give conditions for bifurcation to a low-symmetric phase. An equivalent approach would be to construct from F the effective Landau expansion $\delta f(y_p)$ in a primary order parameter y_p of a low-symmetric phase by systematically eliminating the remaining parameters $\{y_i\}$. A detailed procedure is given in ref 29. For example, in the case of the N_U−N_{TB} phase transition, we could take for the primary order parameter either $y_1 \equiv r_1$ or $y_3 \equiv p_1$ with the final formulas being insensitive to the choice. Before we start, it proves convenient to introduce the auxiliary variables κ_1 and κ_2

https://dx.doi.org/10.1021/acs.jpcc.0c05711
J. Phys. Chem. C 2020, 124, 22761−22775

$$\kappa_1 = 1 + l_4^2\rho_{4,7}$$
$$\kappa_2 = 2\kappa_1 + \rho_{2,2} + l_2^2\rho_{4,14} + l_3^2\rho_{4,6} \quad (30)$$

and relative phases χ_1 and χ_2

$$\chi_1 = \phi_1 - \phi_p$$
$$\chi_2 = \phi_2 - 2\phi_p \quad (31)$$

which simplify the free energy and consequently also bifurcation formulas.

Bifurcation Conditions for I–N_{TB} Phase Transition. Bifurcation conditions for a phase transition from the isotropic phase to the nematic twist–bend phase can be written down as an equation connecting t_P and t_Q

$$a \equiv a(t_P, t_Q) = 2(k^2 + t_P) - \frac{e_P^2 k^2 \sin^2(\chi_1)}{2\kappa_2 k^2 + 4t_Q} = 0 \quad (32)$$

If we permit the k-vector and χ_1 to vary, the bifurcation temperature $t_{P,I-TB}$ from the isotropic to nematic twist–bend phases will be the maximal t_P, fulfilling the condition 32. Solving eq 32 for t_P and maximizing with respect to k and χ give the bifurcation values for k, $\sin(\chi_1)$, and t_P. They read

$$k_{I-TB}^2 = \max\left(0, \frac{\sqrt{t_Q}|e_P|}{\sqrt{2}|\kappa_2|} - \frac{2t_Q}{\kappa_2}\right), \quad \text{for } t_Q > t_{NI} > 0,\ \kappa_2 > 0$$
$$\sin(\chi_{1,I-TB})^2 = 1$$
$$t_{P,I-TB} = \begin{cases} 0 & \text{for } k_{I-TB} = 0 \\ \dfrac{e_P^2 + 8t_Q - 4\sqrt{2}\sqrt{t_Q}|e_P|}{4\kappa_2} & \text{for } k_{I-TB} > 0 \end{cases} \quad (33)$$

where $t_{NI} > 0$ is the isotropic-uniaxial nematic transition temperature. Using formalism of ref 29, one can also show that the a-term, eq 32, is actually the leading coefficient in the Landau expansion of the free energy of the N_{TB} phase about the reference I phase in the primary order parameter p_1

$$\Delta f_{I-TB} = \frac{1}{2!}a p_1^2 + \frac{1}{4!}b p_1^4 + \frac{1}{6!}c p_1^6 + \ldots \quad (34)$$

Generally, the nonzero value k_{I-TB} of the k-vector at the bifurcation point ($e_P^2 > 8t_Q$) indicates that the I–N_{TB} phase transition is, at least weakly, first order. It can be classified as an example of weak crystallization introduced by Kats et al.,[41] with fluctuations that should be observed near the $k = k_{I-TB}$ sphere. Interestingly, for $k = k_{I-TB} = 0$, a direct inspection of higher order terms of the expansion 34 shows that $b = 24a_d - \frac{\lambda^2}{t_Q}$ can change sign for sufficiently large λ. That is, for $c > 0$, the I–N_{TB} transition can be first order ($a = 0$, $b < 0$), second order ($a = 0$, $b > 0$), or tricritical ($a = 0$, $b = 0$).

Bifurcation Conditions for N_U–N_{TB} Phase Transtition. Bifurcation conditions from N_U to N_{TB} expressed in terms of an equation connecting t_P and x_0 read:

$$a \equiv a(t_P, x_0) = 2\left(k^2 + t_P + \frac{\lambda x_0}{\sqrt{6}}\right) - \frac{3e_P^2 \sin^2(\chi_1)}{6\kappa_2 + x_0(\sqrt{6}\kappa_3 + \kappa_4 x_0)} = 0 \quad (35)$$

where $\kappa_3 = \rho_{3,4} - 4\rho_{3,7}$ and $\kappa_4 = 5\rho_{4,7} + 8\rho_{4,15}$ and x_0 is the nematic order parameter calculated from the minimization of f_{Qb} in the uniaxial nematic phase. For fixed t_Q (x_0), the bifurcation temperature corresponds to the maximal t_P, fulfilling the condition of $a = 0$, eq 35, where the maximum is taken over k and χ_1. It yields

$$t_{P,N-TB} = -\frac{\lambda x_0}{\sqrt{6}} + \frac{3e_P^2}{2(6\kappa_2 + \sqrt{6}\kappa_3 x_0 + \kappa_4 x_0^2)} \quad (36)$$

for $k = 0$ and $\sin^2(\chi_1) = 1$. As previously for the I–N_{TB} phase transition, eq 32, the a-term, eq 35, is the leading coefficient in Landau expansion of the free energy of the N_{TB} phase about the reference N_U phase in the primary order parameter p_1:[29] $\Delta f_{N-TB} = \frac{1}{2!}a p_1^2 + \frac{1}{4!}b p_1^4 + \frac{1}{6!}c p_1^6 + \ldots$. A direct inspection of this expansion shows that the N_U–N_{TB} transition can be first order ($a = 0$, $b < 0$, $c > 0$), second order ($a = 0$, $b > 0$, $c > 0$), or tricritical ($a = 0$, $b = 0$, $c > 0$). Our analysis in the next section shows that for the case of CB7CB, the predicted N_U–N_{TB} transition is weakly first order. The tricritical conditions for I–N_{TB} and N_U–N_{TB} phase transitions will be studied in detail elsewhere.

Bifurcations to Globally Polar Phases. In a similar way, we can derive the bifurcation conditions for phase transitions from I, N_U, and N_{TB} to globally polar structures listed in Table 1. It reads

$$a = 2t_P - 2\sqrt{\frac{2}{3}}\lambda x_0 + 4a_d p_1^2 = 0 \quad (37)$$

where $x_0 = p_1 = 0$ for I–$N_{U,p}$ bifurcation, $p_1 = 0$ for N_U–$N_{U,p}$ bifurcation, and both x_0 and p_1 are nonzero when bifurcation takes place from N_{TB} to $N_{TB,p}$. Now, the parameter a is the leading coefficient of Landau expansion $\Delta f_p = \frac{1}{2!}a v_0^2 + \frac{1}{4!}b v_0^4 + \frac{1}{6!}c v_0^6 + \ldots$ in v_0–the primary order parameter for phase transitions to polar structures. Given the form of the expansion for f_P, eq 27, the tricritical point can only be found for the N_{TB}–$N_{TB,p}$ phase transition.

RESULTS AND DISCUSSION

Estimates of Model Parameters from Experimental Data for CB7CB. Before we explore relative stability of the nematic phases given in Table 1, we estimate some of the material parameters entering the expansion 10 from experimental data in the uniaxial nematic phase. This will allow us to study properties of N_{TB} with only a few adjustable parameters. Indeed, nearly all of the parameters of the purely nematic parts the bulk $\tilde{f}_{Qb}$ and the elastic $\tilde{f}_{Qel}$ can be correlated with the existing data in the uniaxial nematic phase. The N_U phase usually appears stable at higher temperatures and N_U–N_{TB} phase transition is observed as temperature is lowered.

The very first compound shown to exhibit the stable nematic and twist–bend nematic phase was the liquid crystal dimer 1″,7″-bis(4-cyanobiphenyl-4′-yl)heptane, abbreviated as CB7CB.[5−7] This compound is constituted of two 4-cyanobiphenyls (CB) linked by an alkylene spacer (C_7H_{14}). Currently, it is one of the best-studied examples with stable N_{TB}. In particular, Babakhanova et al.[20] have carried out a series of experiments for this mesogen in the uniaxial nematic phase. They determined the temperature variation of the nematic order parameter $\tilde{S}$ (see eq 1), the temperature variation of the Frank elastic constants K_{ii} (i = 1, 2, 3), the nematic–isotropic transition temperature T_{NI}, the nematic twist–bend–nematic transition temperature $T_{N_{TB}N}$. An interesting fact is that the twist–bend nematic phase formed by CB7CB can be super-

https://dx.doi.org/10.1021/acs.jpcc.0c05711
J. Phys. Chem. C 2020, 124, 22761−22775

cooled to about 304.15 K[5] and then, there is a glass transition at approximately 277.15 K.[42] We use the data presented in Table S1 to estimate some of the parameters of extended LdeG theory.

Bulk Part. Under the assumption that $\tilde{\mathbf{Q}}$ is uniaxial and positionally independent (eq 1 with $\hat{\mathbf{n}}(\tilde{\mathbf{r}})$ = const.), the order parameter $\tilde{S}$ can be determined from the minimum of the free-energy density $\tilde{f}_{\mathrm{Qb}}$, eq 11, which becomes reduced to that of the uniaxial nematic phase

$$\tilde{f}_{\mathrm{Qb}} = \frac{2}{3}a_{0\mathrm{Q}}(\Delta t + \Delta t_{\mathrm{NI}})\tilde{S}^2 - \frac{2}{9}b\tilde{S}^3 + \frac{4}{9}c\tilde{S}^4 + \frac{4}{27}d\tilde{S}^5 + \frac{4}{81}f\tilde{S}^6 \tag{38}$$

Now, from the necessary condition for minimum, $\partial\tilde{f}_{\mathrm{Qb}}/\partial\tilde{S} = 0$, solved for $T(\tilde{S})$, we determine the ratios $b/a_0 = \tilde{b}$, $c/a_0 = \tilde{c}$, $d/a_0 = \tilde{d}$, and $f/a_0 = \tilde{f}$ by fitting $\{\tilde{S}, T(\tilde{S})\}$ to the experimental data of Babakhanova et al.[20] Independently, the scaling factor a_0 can be estimated from the latent heat per mole $\Delta H_{\mathrm{NI}} = T_{\mathrm{NI}}(\partial\tilde{f}_{\mathrm{Qb}}/\partial T)_{T\to T_{\mathrm{NI}}^-}$ for the nematic−isotropic phase transition.[43] It reads

$$a_0 = \frac{a_{0\mathrm{Q}}}{T_{\mathrm{NI}}} = \frac{3\Delta H_{\mathrm{NI}}(2\tilde{S}_{\mathrm{NI}}(24\tilde{c} + \tilde{S}_{\mathrm{NI}}(15\tilde{d} + 8\tilde{f}\,\tilde{S}_{\mathrm{NI}})) - 9\tilde{b})}{2\tilde{S}_{\mathrm{NI}}T_{\mathrm{NI}}(9\tilde{b}\tilde{S}_{\mathrm{NI}} + 10\tilde{d}\tilde{S}_{\mathrm{NI}}^3 + 8\tilde{f}\,\tilde{S}_{\mathrm{NI}}^4 - 36T_{\mathrm{NI}} + 36T^*)} \tag{39}$$

where $\tilde{S}_{\mathrm{NI}}$ is the nematic order parameter at the uniaxial nematic−isotropic phase transition. For overall consistency, a_0 has been multiplied onward by $\rho_{\mathrm{C}} = \rho/M_{\mathrm{w}} \approx 2.22 \times 10^3$ mol/m^3, which is the ratio of the mass density ($\rho \approx 10^3$ kg/m^3) to the relative molecular weight of CB7CB ($M_{\mathrm{w}} \approx 0.45$ kg/mol), yielding the value 6.88×10^4 J m^{-3} K^{-1}. Thanks to this operation, it was possible to express all expansion coefficients in units J m^{-3}. Figure 3 depicts results of fitting to experimental data, whereas numerical values of the parameters are gathered in Table S2. Please observe that the expansion parameter e couples to a purely biaxial part and therefore, it cannot be estimated from the data in $\mathrm{N_U}$.

Flexopolarization Renormalized Elasticity of Uniaxial Nematics. It is important to realize that although (flexo)-polarization terms 20, 21 vanish in the uniaxial nematic phase, any local deformation of the alignment tensor induces deformation of $\tilde{\mathbf{P}}$ because of the flexopolarization coupling $\varepsilon_{\mathrm{P}} \neq 0$. Such deformations effectively renormalize elastic constants $L_m^{(n)}$ in ordinary nematic phases. The effect cannot be neglected if we intend to estimate $L_m^{(n)}$ from experimental data. A mathematical procedure of taking into account such deformations in the $\mathrm{N_U}$ phase is to minimize the free energy, eq 10, over Fourier modes of the polarization field for given fixed Fourier modes of the alignment tensor. Assuming that deformation $\tilde{\mathbf{Q}}(\tilde{\mathbf{r}})$ is small and slowly varying, we obtain with this procedure the $\tilde{\mathbf{Q}}$-induced deformation of $\tilde{\mathbf{P}}(\tilde{\mathbf{r}})$ expressed in terms of Fourier modes, which when transformed back to the real space take the form of a series in $Q_{\alpha\mu}$ and $Q_{\alpha\mu,\mu}$ and in higher order derivatives of $Q_{\alpha\mu}$. The relevant terms are

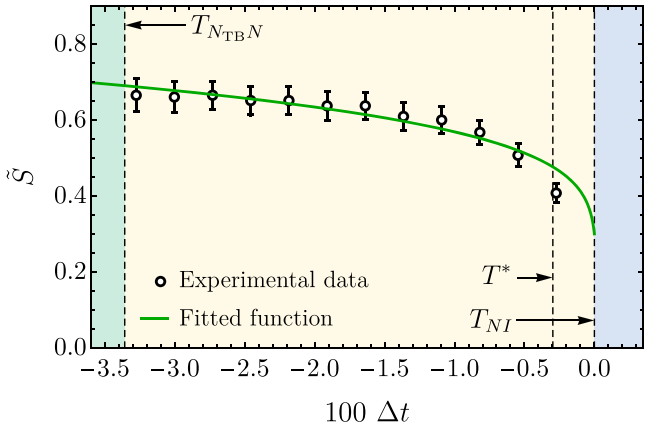

Figure 3. Experimental data from ref 20 representing the temperature dependence of $\tilde{S}$ in the uniaxial nematic phase of CB7CB. The green line illustrates the effect of fitting predictions of the theory 38 to the data. T^* represents the maximal supercooling temperature of the isotropic phase. Our fit is carried out by taking as an *ansatz* the experimentally known value of T_{NI} and T^*. Then, $\tilde{S}_{\mathrm{NI}}$ for CB7CB is estimated from our fitted function. If we compromise the agreement of T_{NI} and T^* with experimental data, a better fit can be obtained for $\tilde{S}$ close to the transition temperature without affecting the one in the vicinity of $\mathrm{N_U}$−$\mathrm{N_{TB}}$.

$$\tilde{P}_\alpha(\tilde{\mathbf{r}}) = \frac{\varepsilon_{\mathrm{P}}}{2a_{\mathrm{P}}}\tilde{Q}_{\alpha\mu,\mu} + \frac{\varepsilon_{\mathrm{P}}\Lambda_{\mathrm{QP}}}{2a_{\mathrm{P}}^2}\tilde{Q}_{\alpha\beta}\tilde{Q}_{\beta\mu,\mu} + \frac{\varepsilon_{\mathrm{P}}\Lambda_{\mathrm{QP}}^2}{2a_{\mathrm{P}}^3}\tilde{Q}_{\alpha\lambda}\tilde{Q}_{\lambda\beta}\tilde{Q}_{\beta\mu,\mu} + \ldots \tag{40}$$

Substituting eq 40 back to $\tilde{f}_{\mathrm{P}}$ and $\tilde{f}_{\mathrm{QP}}$, we obtain effective elastic contributions expressed in terms of only $\tilde{Q}_{\alpha\beta}$ and $\tilde{Q}_{\gamma\mu,\mu}$. When added to $\tilde{f}_{\mathrm{Qel}}$, they give an effective elastic free energy of uniaxial and biaxial nematics with $L_m^{(n)}$ being replaced by $L_{m,\mathrm{eff}}^{(n)}$, where relevant $L_m^{(n)}$'s are

$$L_2^{(2)} \to L_{2,\mathrm{eff}}^{(2)} = L_2^{(2)} - \frac{\varepsilon_{\mathrm{P}}^2}{4a_{\mathrm{P}}}$$

$$L_3^{(3)} \to L_{3,\mathrm{eff}}^{(3)} = L_3^{(3)} - \frac{\Lambda_{\mathrm{QP}}\varepsilon_{\mathrm{P}}^2}{4a_{\mathrm{P}}^2}$$

$$L_6^{(4)} \to L_{6,\mathrm{eff}}^{(4)} = L_6^{(4)} - \frac{\Lambda_{\mathrm{QP}}^2\varepsilon_{\mathrm{P}}^2}{4a_{\mathrm{P}}^3} \tag{41}$$

An important physical distinction between the bare constant $L_m^{(n)}$ and the renormalized constant $L_{m,\mathrm{eff}}^{(n)}$ is of the same sort as the one between renormalized and bare Frank elastic constants, as discussed by Jákli, Lavrentovich, and Selinger:[3] $L_m^{(n)}$ gives the energy cost of $\tilde{Q}_{\alpha\beta,\gamma}$ deformations if we constrain $\tilde{P}_\alpha = 0$ during the deformation, while $L_{m,\mathrm{eff}}^{(n)}$ relaxes to its optimum value during the deformation. Assuming that major contribution to flexopolarization is of the entropic, excluded volume type, any realistic experiment to measure elastic constants should not put constraints on the polar field $\tilde{\mathbf{P}}$ but rather allows it to relax. In this case, which is analysed here, $L_{m,\mathrm{eff}}^{(n)}$ is the relevant contribution to the elastic constants in eq 14.

Elastic Part. In the hydrodynamic limit where spatial dependence of $\tilde{S}$ is disregarded and $\tilde{\mathbf{Q}}$ is given by 1, the elastic free energy $\tilde{f}_{\mathrm{Qel}}$ turns into the OF free-energy density of the

https://dx.doi.org/10.1021/acs.jpcc.0c05711
J. Phys. Chem. C 2020, 124, 22761−22775

director field $\mathbf{n}(\tilde{\mathbf{r}})$, eq 2, with K_{11}, K_{22}, and K_{33} being polynomials in $\tilde{S}$[28]

$$K_{ii} = K_{ii}^{(2)}\tilde{S}^2 + K_{ii}^{(3)}\tilde{S}^3 + K_{ii}^{(4)}\tilde{S}^4 \qquad (i = 1, 2, 3) \tag{42}$$

The coefficients, $K_{ii}^{(n)}$, are functions of $L_j^{(n)}$,[28,30] fulfilling the splay−bend degeneracy relation in the second order: $K_{11}^{(2)} = K_{33}^{(2)}$. For completeness, they are given in the Supporting Information. As it turns out, $K_{ii}^{(n)}$ with $n = 2, 3, 4$ along with flexopolarization renormalization 41 is sufficient to obtain a good fit of eq 42 to experimentally observed K_{ii} for CB7CB.[20] Importantly, they also provide an estimate for the (flexo)polar couplings ε_p and Λ_{QP}. In finding $K_{ii}^{(n)}$, we use the $\tilde{S}(T)$ fit obtained from the analysis of the bulk free energy, which is a prerequisite to have a consistent theory of the uniaxial nematic phase for this compound. Results of fitting are gathered in Table S2. Finally, as the number of relevant couplings $L_\alpha^{(n)}$ ($n = 3, 4$), eq 14, equals that of $K_{ii}^{(n)}$, we can correlate $L_\alpha^{(n)}$ with $K_{ii}^{(n)}$ using the results of the Supporting Information and of ref 28. It yields

$$\begin{aligned}
&L_1^{(2)} + \lambda_4{}^2 L_7^{(4)} = \frac{1}{4}K_{22}^{(2)}\\
&L_2^{(2)} + \lambda_2{}^2 L_{14}^{(4)} + \lambda_3{}^2 L_6^{(4)} - \frac{\varepsilon_p{}^2}{4a_p} = \frac{1}{2}(K_{11}^{(2)} - K_{22}^{(2)})\\
&L_2^{(3)} = \frac{1}{2}(K_{11}^{(3)} - 3K_{22}^{(3)} + 2K_{33}^{(3)})\\
&L_3^{(3)} - \frac{\Lambda_{QP}\varepsilon_p{}^2}{4a_p{}^2} = \frac{1}{2}(2K_{11}^{(3)} - 3K_{22}^{(3)} + K_{33}^{(3)})\\
&L_4^{(3)} = \frac{3}{2}K_{22}^{(3)}\\
&L_6^{(4)} - \frac{\Lambda_{QP}{}^2\varepsilon_p{}^2}{4a_p{}^3} = \frac{3}{10}(4K_{11}^{(4)} - 3K_{22}^{(4)} - K_{33}^{(4)})\\
&L_7^{(4)} = \frac{9}{10}K_{22}^{(4)}\\
&L_{14}^{(4)} = -\frac{3}{10}(K_{11}^{(4)} + 3K_{22}^{(4)} - 4K_{33}^{(4)})
\end{aligned} \tag{43}$$

Results of fitting of $L_\alpha^{(n)}$, eq 14, obeying stability ansatz 15 to experimental data for CB7CB are given in Table S2. The quality of fit is displayed in Figure 4.

Predictions for the Nematic Twist−Bend Phase of CB7CB-like Compounds. Within this section, we explore the relative stability of the UDS, listed in Table 1, for the model 24 with parameters (estimated in previous sections), which are gathered in Table S3. We limit ourselves to the temperature interval where the N_{TB} phase appears stable in the experiment (Table S4).

The temperatures t_p and t_Q are connected with the absolute temperature T of the system studied (see eqs 12, 20, and 22). Because $a_{0P} > 0$, $a_{0Q} > 0$, $T^* > T_p$, and $T > T_p$, any straight line in the $\{t_Q, t_p\}$ plane with a positive slope and negative t_Q-intercept represents a permissible physical system with no polar order for $\tilde{\mathbf{Q}} = 0$. Thus, we present the phase diagrams in the general $\{t_Q, t_p\}$ plane for a broader view. In our case, the experimentally related line has the form:

$$t_p = 4.13t_Q + 8.29 \tag{44}$$

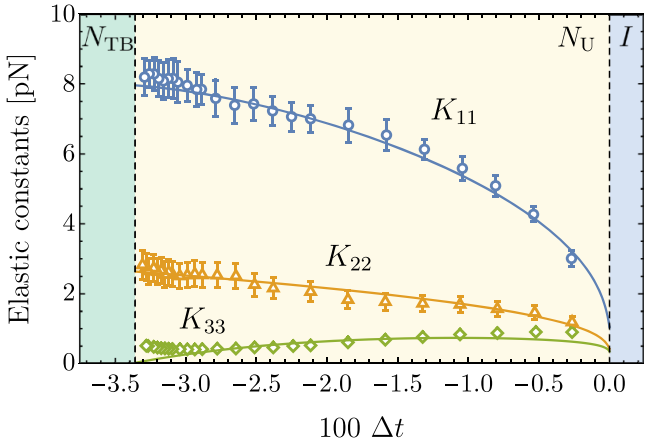

Figure 4. Temperature dependence of elastic constants acquired from ref 20. Continuous lines depict the adopted approach for elastic constants within the model. Note that the model cannot explain a slight increase in K_{33} in the vicinity of the N_U−N_{TB} phase transition.

Results of our in-depth analysis profoundly reduced the number of adjustable parameters for CB7CB-like compounds to solely four (λ, e_p, a_d, and e_b). From considerations related to the elastic constants, Table S2, it turns out that Λ_{QP} (*ipso facto* λ), responsible for globally polar structures, is negligible, that is, $\sqrt{|\lambda|}/e_p \approx 10^{-13}$. Thus, we set $\lambda = 0$. Onward, we take $e_p = 7.1$ and $a_d = 0.75$ as the best values to reproduce the temperature dependance of k. For the bulk biaxial parameter e_b, we take two values: $e_b = 0$ and $e_b = 1/6$. If we recall eq 25, there is a term $e_b(I_2{}^3 - 6I_3{}^2) + I_3{}^2$. If we set $e_b = 0$, it reduces to $I_3{}^2$; on the other hand, when we set $e_b = 1/6$, we have only $I_2{}^3/6$. In the following discussion, the first scenario ($e_b = 0$) will be referred to as theory $(I_3{}^2)$ and second one as theory $(I_2{}^3)$. The $(I_3{}^2)$ theory will enhance phase biaxiality because of its tendency to lower the equilibrium value of the w parameter, eq 9, while the $(I_2{}^3)$ theory is promoting the $w = \pm 1$ states through cubic and fifth-order terms in 25.[32] In this latter case, the biaxiality of N_{TB} can only be induced by the elastic terms.

Figure 5a−f depict phase diagrams combined with density maps of k, θ, w, r_1, r_2, and p_1, which are outcomes of theory $(I_3{}^2)$. In the analyzed case, being consistent with the experiment, stable, apart from isotropic, is the uniaxial nematic phase and the twist−bend nematic phase. The dashed green curve denotes numerically determined phase transitions and the red continuous curve marks the results from the bifurcation analysis. Vertical, dashed white lines designate the temperature span of N_U stability (experimental) mapped on t_Q (see Table S4). The purple straight line described by eq 44 represents the phase transition sequence $I \leftrightarrow N_U \leftrightarrow N_{TB}$ based on the CB7CB data from ref 20. From points lying on this line, we have attained information about the behavior of the pitch (p), tilt angle (θ), and nematic order parameter ($\tilde{S}$) in N_{TB}, alongside the insight into the N_{TB}'s biaxiality parameter (w) and the remaining order parameters (r_1, r_2, and p_1) (see Figure 6a−f). With regard to the w parameter, in the literature, there are no available results concerning the biaxiality of N_{TB}; thus, it is hard to compare. Nevertheless, our model permits to estimate the span and magnitude of the effect on experimentally measurable parameters.

We set together results of our model with available experimental data concerning the pitch p (Figure 6a[7,44]), tilt angle θ (Figure 6b[45−50]), and nematic order parameter $\tilde{S}$ (Figure

https://dx.doi.org/10.1021/acs.jpcc.0c05711
J. Phys. Chem. C 2020, 124, 22761−22775

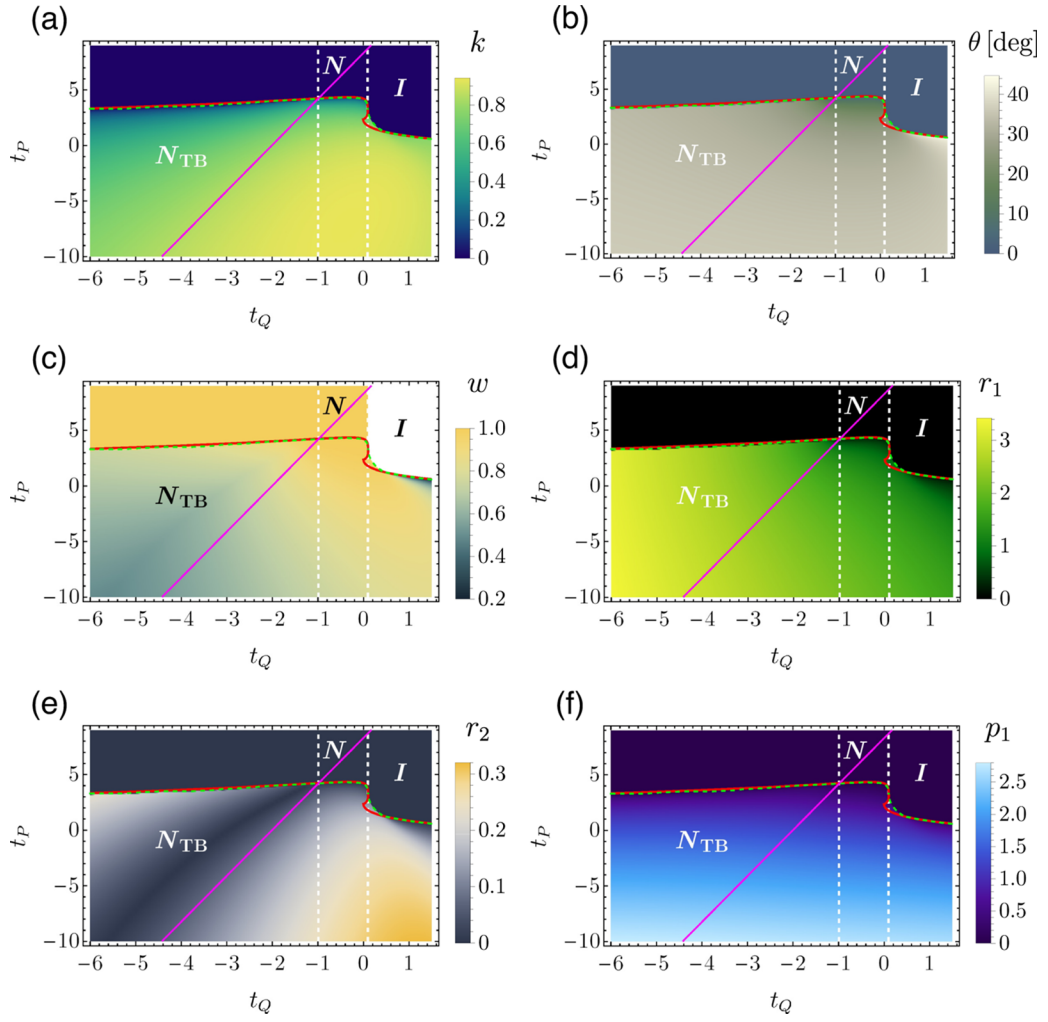

Figure 5. Phase diagram combined with density map of the wave vector k (a), tilt angle θ (b), biaxiality parameter w (c), and mode's amplitudes: r_1 (d), r_2 (e) and p_1 (f) within the theory (I_3^2). The red continuous curve marks the bifurcation between N ↔ N_{TB} and I ↔ N_{TB}, whereas the dashed green curve outlines the numerical results. The magenta line (described by eq 44) reflects the phase sequence associated directly with the experimental data for CB7CB. Vertical, dashed white lines designate the temperature span of N_U stability (experimental) mapped on t_Q (see Table S4).

6c[20,49−51]). At the transition temperature from N_U to N_{TB}, the pitch length is *ca.* 54 nm and with decreasing temperature, it saturates at the level of *ca.* 8 nm (Figure 6a). As one can see, it goes fairly well with the experimental data. Within the literature, the methodology regarding the pitch measurements for CB7CB is consistent, that is, all indicate that the pitch value reaches plateau at *ca.* 8 nm,[6,7,44] in contradiction to measurements of θ and $\tilde{S}$.

Such span of experimental data for θ, Figure 6b, originates from the adopted method of determination and sample treatment. In refs,[45,46,48] birefringence measurements were employed; however, the choice of the region in which they were taken varied across the aforementioned papers (see discussion in ref 46). In refs 49 and 50, the data regarding the conical tilt angle were extracted from X-ray methods, wherein in ref 49, it was small/wide angle X-ray scattering (SAXS/WAXS) and in ref 50 X-ray diffraction (XRD). In turn, the conical tilt angle from ref 47 was determined *i.a.* from ^{2}H nuclear magnetic resonance (NMR) quadrupolar splittings of CB7CB-d_4. Similar to the tilt angle, discrepancies between the data related to the order parameter, Figure 6c, arise from the method of acquisition. In ref 20, it was extracted from diamagnetic anisotropy measurements, in ref 49, from SAXS, in ref 50, from XRD, and in refs 50 and 51, from polarized Raman spectroscopy (PRS). As one can see, data from ref 20 stand out from the rest of the data (Figure 6c), although it was the only source that provided simultaneously the data for the temperature dependence of the orientational order parameter and elastic constants.

One can see that results of our model are generally in a very good agreement with experimental results, perhaps except an immediate vicinity of the N_U−N_{TB} phase transition where fluctuations, not included in the present analysis, may play a role. Predictions concerning the effect of intrinsic, molecular biaxiality on N_{TB} seem interesting. Although the pitch, $\tilde{S}$, and p_1 are practically insensitive to w, the remaining observables are affected. In particular, for the tilt angle, the green continuous line associated with $e_b = 0$ (I_3^2 model) fits well in between the data from ref 45 (blue circles) and ref 48 (yellow squares), whereas the red dashed line, associated with the weakly biaxial case (I_2^3 model), markedly departs from the abovementioned experimental data. Based on the results of Babakhankova et al.,[20] we can conclude that biaxiality of N_{TB}, initially small at the N_U−N_{TB} phase transition, considerably increases on departing from the transition temperature (green line in Figure 6d). Figure 6e illustrates the behavior of the order parameters r_1, r_2, and p_1 in the N_{TB} phase of CB7CB, where the ratio $\sigma = r_1/r_2$ can be

https://dx.doi.org/10.1021/acs.jpcc.0c05711
J. Phys. Chem. C 2020, 124, 22761−22775

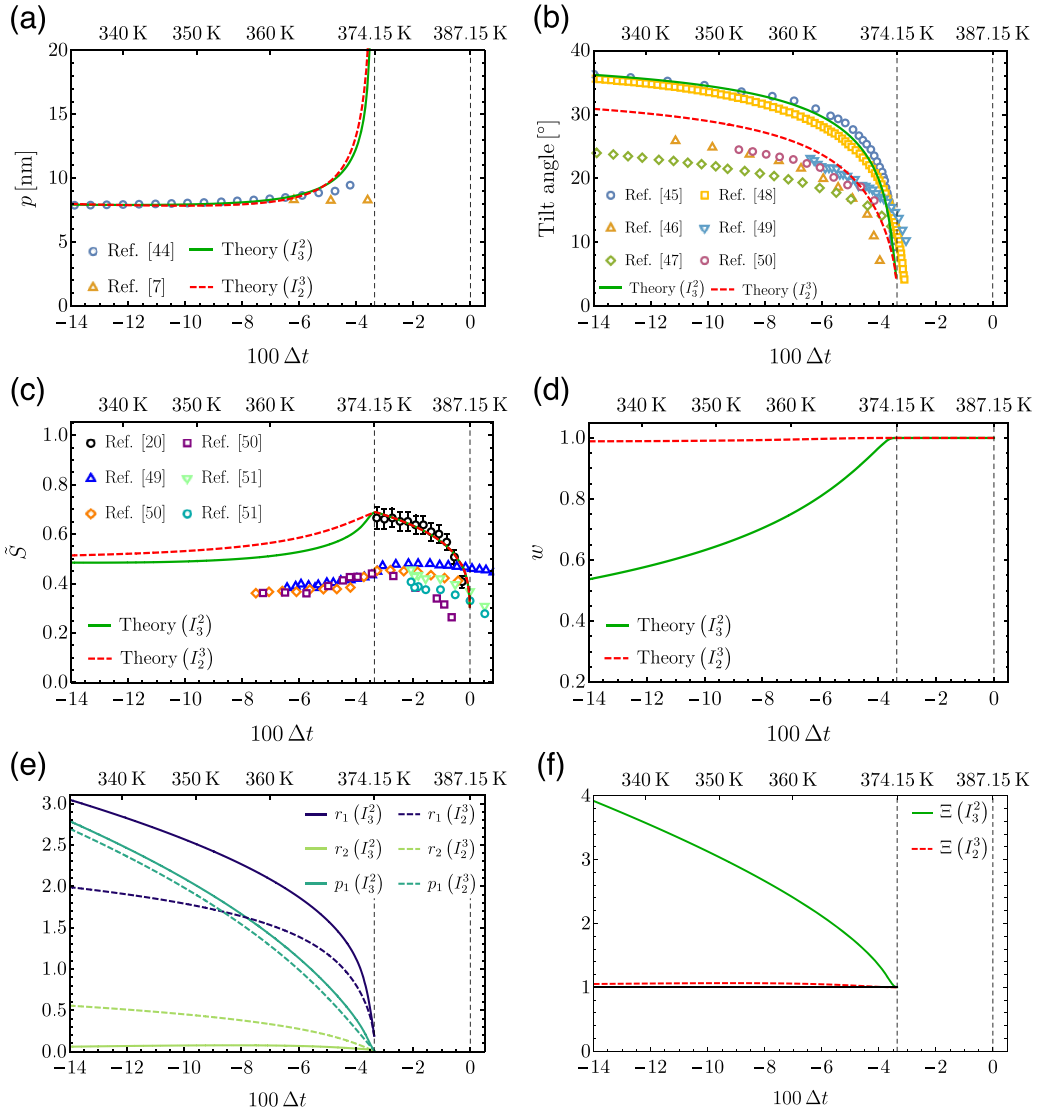

Figure 6. Comparison between experimental data (hollow points) and theoretical predictions (continuous green and dashed red line) for CB7CB's N_{TB}. (a) Temperature dependence of the N_{TB}'s pitch p, (b) tilt angle θ, and (c) order parameter $\tilde{S}$. (d) Plot depicts the behavior of the biaxiality parameter w and the plot of (e) mode's amplitudes r_1, r_2, and p_1 as a function of temperature in the range of N_{TB} stability. (f) Plot illustrates the temperature behavior of the relevant factor, parameterizing the relative magnitudes of intensities of two leading harmonics of the dispersion tensor that contribute to the resonant soft X-ray scattering (RSoXS).[52] All the data are drawn with respect to the multiplied by factor 100 reduced temperature Δt, whereas key temperatures, corresponding to given Δt, are designated above each plot in absolute temperature T.

correlated with data acquirable from resonant soft X-ray scattering (RSoXS).[44,53,54] In order to make this correlation, we translated our formalism into the one presented in ref 52. Thanks to that, we could tie the results for σ with experimentally measurable scattering intensities through the following formula

$$\Xi = -\frac{1}{2} + \frac{3\sigma}{2\sigma\cos(2\theta) + 4\sin(2\theta)} \tag{45}$$

where $\Xi = f_1/f_2$ and θ is the conical tilt angle. The value of the parameter Ξ determines the intensity of the $2q_0$ peak (half-pitch band) with respect to the intensity of the q_0 peak (full-pitch band) in the N_{TB} phase, where $q_0 = 2\pi/p$ is the magnitude of the wave vector of the heliconical deformation with the pitch p. As it was stated in ref 52, if $\Xi \geq 1$, then the intensity of the $2q_0$ peak is approximately 2 orders of magnitude lower than the intensity of the q_0 peak and further strongly decreases with increasing Ξ. On the other hand, if $\Xi < 1$, then the intensity of the $2q_0$ peak escalates rapidly. As one can see in Figure 6f, which illustrates the temperature dependence of Ξ for both theories $I_3{}^2$ and $I_2{}^3$, all the data obey the relation $\Xi \geq 1$, indicating a significant weakness of the $2q_0$ peak. Interestingly, although for $I_2{}^3$ theory, the relative magnitude of the intensities should roughly differ by 2 orders of magnitude irrespective of the temperature, the $I_3{}^2$ model predicts further strong reduction in the relative intensity with temperature. To the best of our knowledge, the $2q_0$ signal has not been detected so far in any of the examined N_{TB}-forming compounds.[44,53−55]

CONCLUSIONS

The understanding of self-organization in the twist−bend nematic (N_{TB}) phase is at the forefront of soft matter research worldwide. This new nematic phase develops structural chirality in the isotropic and uniaxial nematic phases, despite the fact that the molecules forming the structure are chemically *achiral*. Currently existing experimental data are in favor of the theory that the N_U−N_{TB} phase transition is driven by the flexopolariza-

https://dx.doi.org/10.1021/acs.jpcc.0c05711
J. Phys. Chem. C 2020, 124, 22761−22775

tion mechanism. According to this theory, deformations of the director induce a local polar order which, in turn, renormalizes the bend elastic constant to a very small value relative to other elastic constants, eventually leading to the twist−bend instability. It is dictated by the term coupled with $[L_2^{(2)}]$ (eq 14), which changes sign from positive to negative at the bifurcation temperature between the nematic and twist−bend nematic.

However, a fundamental description of orientational properties of nematics based on minimal coupling LdeG theory of flexopolarization suggests that softening of K_{33} does not need to be a universal mechanism. Even when both K_{11} and K_{33} are simultaneously reduced because of splay−bend degeneracy (inherent to the minimal coupling LdeG expansion), the N_{TB} phase can still become absolutely stable among all possible one-dimensional periodic structures. Because this case has not been observed experimentally to date, an important question that arises is whether the flexopolarization mechanism is indeed sufficient to explain the experimental observations at the level of "first principles" LdeG theory of the orientational order. To address this issue, we proposed generalization of mesoscopic LdeG theory of nematics, where higher order elastic terms of the alignment tensor are taken systematically into account, in addition to the lowest order flexopolarization coupling.

We demonstrated that the experimental observations involving the nematic twist−bend phase and the related uniaxial nematic phase can be explained if we generalize minimal coupling theory to the level where the properties of the high-temperature uniaxial nematic phase are properly accounted for. Especially, the constructed generalized free-energy density is in line with experimentally observed temperature variation of the orientational order parameter and the Frank elastic constants, except slight pretransitional increase in K_{22} and K_{33} on approaching the $N-N_{TB}$ phase transition. The origin of this pretransitional elastic response is still not fully understood. Babakhanova et al.[20] attributed increase in the elastic constants to the formation of clusters with periodic twist−bend modulation of the director, in analogy to similar pretransitional increase in K_{22} and K_{33} near the nematic-to-smectic A phase transition.[56−58] Shi et al.[59] in their Monte Carlo simulations of an augmented Lebwohl−Lasher lattice model predicted the temperature behavior of K_{33} to be in qualitative accordance with experimental results. Comparison of Figures 2f and 7 in ref 59 suggests that a probable cause of this pretransitional anomaly of elasticity is flexopolarization-induced short-range polar ordering in the uniaxial nematic phase. In the present model, none of the abovementioned scenarios are included. It would require a phenomenological theory with fluctuating $\tilde{\mathbf{Q}}$ and $\tilde{\mathbf{P}}$ fields, which is far beyond our ground-state analysis.

Our generalized theory of uniformly distorted nematics extends the elastic part of LdeG by additional two terms of third order. The added elastic terms are the only independent ones for the UDSs and various UDSs can become minimizers of the free energy, including the nematic twist−bend. This conclusion follows directly from the bifurcation analysis and the observation that the remaining four independent elastic terms of third order, not included in the theory, can always be written in such a way that they vanish for UDSs. It is worth noticing that only one more term is generally needed to extend the studies of the UDS class to *all possible* one-dimensional distortions of the alignment tensor. This sort of hierarchy between various elastic invariants indicates that the constructed theory can also serve as a starting point in seeking different mechanisms of softening of the nematic elastic constants. This can potentially lead to the discovery of new classes of modulated nematic structures.

The numerical analysis of the model quite well reproduces measured quantities for the N_U and N_{TB} phases of the CB7CB-like mesogens and gives numerical estimates for its constitutive parameters including otherwise difficult to access (flexo) polarization couplings. Overall, the N_{TB} phase is predicted to be biaxial with theoretical support that major contribution to the phase biaxiality can originate from the bulk term(s) in the free energy. Although the phase transitions to N_{TB} are weakly first order for CB7CB, the theory permits the transitions to N_{TB} be second order with tricritical $I-N_{TB}$ and N_U-N_{TB} points.

Finally, very recent theories of Čopič and Mertelj[60] and Anzivion et al.,[61] also based on **Q**-tensor LdeG expansion, address the issue of relative stability of uniaxial, twist−bend, and splay−bend (N_{SB}) nematic phases for thermotropic bent-core-like materials[60] and for lyotropic colloidal suspensions of bent rods.[61] Their theory uses minimal coupling expansion[12,24] extended to include one of the cubic invariants (eq S.2) that breaks splay−bend degeneracy. Because their thermodynamic potentials are unbounded from below for the general $\tilde{\mathbf{Q}}$-tensor, they can only study uniaxial tensors, eq 1, of $\tilde{S} \geq 0$ to model twist−bend and splay−bend nematics, in contrast to our theory which is free of such limitations. They predict a sequence of phase transitions between N, N_{TB}, and N_{SB} with the modulated nematic order being observed upon increasing $\tilde{S}$. Although these predictions are generally consistent with our bifurcation analysis of the $N-N_{TB}$ phase transition, eq 36, a more complex behavior can also be envisaged for nonzero λ, κ_3, and κ_4, if they all are allowed to vary independently.

■ ASSOCIATED CONTENT

Supporting Information

The Supporting Information is available free of charge at https://pubs.acs.org/doi/10.1021/acs.jpcc.0c05711.

Complete expression for elastic free energy of nematic liquid crystals, effective elastic constants, and free energy density of the UDSs. Experimental data, along with numerical results (PDF)

■ AUTHOR INFORMATION

Corresponding Authors

Lech Longa − *Institute of Theoretical Physics, Jagiellonian University, 30-348 Kraków, Poland;* orcid.org/0000-0002-4918-6518; Email: lech.longa@uj.edu.pl

Wojciech Tomczyk − *Institute of Theoretical Physics, Jagiellonian University, 30-348 Kraków, Poland;* orcid.org/0000-0002-7649-3329; Email: wojciech.tomczyk@doctoral.uj.edu.pl

Complete contact information is available at: https://pubs.acs.org/10.1021/acs.jpcc.0c05711

Notes

The authors declare no competing financial interest.

■ ACKNOWLEDGMENTS

This work was partly supported by the grant no. DEC-2013/11/B/ST3/04247 of the National Science Centre in Poland. L.L. acknowledges partial support by the EPSRC grant EP/R014604/1 [The Mathematical Design of New Materials-2019] of the Isaac Newton Institute for Mathematical Sciences,

University of Cambridge, UK. W.T. acknowledges partial support by Marian Smoluchowski Scholarship (KNOW/58/SS/WT/2016) from Marian Smoluchowski Cracow Scientific Consortium "Matter-Energy-Future" within the KNOW grant and by Jagiellonian Interdisciplinary PhD Programme co-financed from the European Union funds under the European Social Fund (POWR.03.05.00-00-Z309/17-00).

REFERENCES

(1) de Gennes, P. G.; Prost, J. *The Physics of Liquid Crystals*, 2nd ed.; Clarendon Press: Oxford, U.K., 1993.
(2) Takezoe, H.; Gorecka, E.; Čepič, M. Antiferroelectric liquid crystals: Interplay of simplicity and complexity. *Rev. Mod. Phys.* **2010**, *82*, 897−937.
(3) Jákli, A.; Lavrentovich, O. D.; Selinger, J. V. Physics of liquid crystals of bent-shaped molecules. *Rev. Mod. Phys.* **2018**, *90*, 045004−045071.
(4) Panov, V. P.; Nagaraj, M.; Vij, J. K.; Panarin, Y. P.; Kohlmeier, A.; Tamba, M. G.; Lewis, R. A.; Mehl, G. H. Spontaneous periodic deformations in nonchiral planar-aligned bimesogens with a nematic-nematic transition and a negative elastic constant. *Phys. Rev. Lett.* **2010**, *105*, 167801−167804.
(5) Cestari, M.; Diez-Berart, S.; Dunmur, D. A.; Ferrarini, A.; de La Fuente, M. R.; Jackson, D. J. B.; López, D. O.; Luckhurst, G. R.; Perez-Jubindo, M. A.; Richardson, R. M.; et al. Phase behavior and properties of the liquid-crystal dimer 1″, 7″-bis(4-cyanobiphenyl-4′-yl) heptane: a twist-bend nematic liquid crystal. *Phys. Rev. E: Stat., Nonlinear, Soft Matter Phys.* **2011**, *84*, 031704−031723.
(6) Borshch, V.; Kim, Y.-K.; Xiang, J.; Gao, M.; Jákli, A.; Panov, V. P.; Vij, J. K.; Imrie, C. T.; Tamba, M. G.; Mehl, G. H.; et al. Nematic twist-bend phase with nanoscale modulation of molecular orientation. *Nat. Commun.* **2013**, *4*, 2635−2642.
(7) Chen, D.; Porada, J. H.; Hooper, J. B.; Klittnick, A.; Shen, Y.; Tuchband, M. R.; Korblova, E.; Bedrov, D.; Walba, D. M.; Glaser, M. A.; et al. Chiral heliconical ground state of nanoscale pitch in a nematic liquid crystal of achiral molecular dimers. *Proc. Natl. Acad. Sci. U.S.A.* **2013**, *110*, 15931−15936.
(8) Mertelj, A.; Cmok, L.; Sebastián, N.; Mandle, R. J.; Parker, R. R.; Whitwood, A. C.; Goodby, J. W.; Čopič, M. Splay nematic phase. *Phys. Rev. X* **2018**, *8*, 041025−041036.
(9) Tuchband, M. R.; Paterson, D. A.; Salamończyk, M.; Norman, V. A.; Scarbrough, A. N.; Forsyth, E.; Garcia, E.; Wang, C.; Storey, J. M. D.; Walba, D. M.; et al. Distinct differences in the nanoscale behaviors of the twist-bend liquid crystal phase of a flexible linear trimer and homologous dimer. *Proc. Natl. Acad. Sci. U.S.A.* **2019**, *116*, 10698−10704.
(10) Srigengan, S.; Nagaraj, M.; Ferrarini, A.; Mandle, R.; Cowling, S. J.; Osipov, M. A.; Pająk, G.; Goodby, J. W.; Gleeson, H. F. Anomalously low twist and bend elastic constants in an oxadiazole-based bent-core nematic liquid crystal and its mixtures; contributions of spontaneous chirality and polarity. *J. Mater. Chem. C* **2018**, *6*, 980−988.
(11) Pająk, G.; Longa, L.; Chrzanowska, A. Nematic twist-bend phase in an external field. *Proc. Natl. Acad. Sci. U.S.A.* **2018**, *115*, E10303−E10312.
(12) Longa, L.; Pająk, G. Modulated nematic structures induced by chirality and steric polarization. *Phys. Rev. E: Stat., Nonlinear, Soft Matter Phys.* **2016**, *93*, 040701−040705.
(13) Archbold, C. T.; Davis, E. J.; Mandle, R. J.; Cowling, S. J.; Goodby, J. W. Chiral dopants and the twist-bend nematic phase-induction of novel mesomorphic behaviour in an apolar bimesogen. *Soft Matter* **2015**, *11*, 7547−7557.
(14) Dawood, A. A.; Grossel, M. C.; Luckhurst, G. R.; Richardson, R. M.; Timimi, B. A.; Wells, N. J.; Yousif, Y. Z. On the twist-bend nematic phase formed directly from the isotropic phase. *Liq. Cryst.* **2016**, *43*, 2−12.
(15) Meyer, R. B. In *Proceedings of the Les Houches Summer School on Theoretical Physics, 1973*, session No. XXV; Balian, R., Weill, G., Eds.; Gordon and Breach Science Publishers, 1976; p 271.
(16) Dozov, I. On the spontaneous symmetry breaking in the mesophases of achiral banana-shaped molecules. *Europhys. Lett.* **2001**, *56*, 247−253.
(17) Oseen, C. W. The theory of liquid crystals. *Trans. Faraday Soc.* **1933**, *29*, 883−899.
(18) Frank, F. C. I. Liquid crystals. On the theory of liquid crystals. *Discuss. Faraday Soc.* **1958**, *25*, 19−28.
(19) Shamid, S. M.; Dhakal, S.; Selinger, J. V. Statistical mechanics of bend flexoelectricity and the twist-bend phase in bent-core liquid crystals. *Phys. Rev. E: Stat., Nonlinear, Soft Matter Phys.* **2013**, *87*, 052503−052513.
(20) Babakhanova, G.; Parsouzi, Z.; Paladugu, S.; Wang, H.; Nastishin, Y. A.; Shiyanovskii, S. V.; Sprunt, S.; Lavrentovich, O. D. Elastic and viscous properties of the nematic dimer CB7CB. *Phys. Rev. E: Stat., Nonlinear, Soft Matter Phys.* **2017**, *96*, 062704−062715.
(21) Cukrov, G.; Golestani, Y. M.; Xiang, J.; Nastishin, Y. A.; Ahmed, Z.; Welch, C.; Mehl, G. H.; Lavrentovich, O. D. Comparative analysis of anisotropic material properties of uniaxial nematics formed by flexible dimers and rod-like monomers. *Liq. Cryst.* **2017**, *44*, 219−231.
(22) Atkinson, K. L.; Morris, S. M.; Castles, F.; Qasim, M. M.; Gardiner, D. J.; Coles, H. J. Flexoelectric and elastic coefficients of odd and even homologous bimesogens. *Phys. Rev. E: Stat., Nonlinear, Soft Matter Phys.* **2012**, *85*, 012701−012704.
(23) Gartland, E. C., Jr. Scalings and limits of Landau-de Gennes models for liquid crystals: a comment on some recent analytical papers. *Math. Model. Anal.* **2018**, *23*, 414−432.
(24) Longa, L.; Trebin, H.-R. Spontaneous polarization in chiral biaxial liquid crystals. *Phys. Rev. A: At., Mol., Opt. Phys.* **1990**, *42*, 3453−3469.
(25) Merkel, K.; Kocot, A.; Vij, J. K.; Shanker, G. Distortions in structures of the twist bend nematic phase of a bent-core liquid crystal by the electric field. *Phys. Rev. E: Stat., Nonlinear, Soft Matter Phys.* **2018**, *98*, 022704−022711.
(26) Mandle, R. J.; Davis, E. J.; Archbold, C. T.; Voll, C. C. A.; Andrews, J. L.; Cowling, S. J.; Goodby, J. W. Apolar bimesogens and the incidence of the twist-bend nematic phase. *Chem.—Eur. J.* **2015**, *21*, 8158−8167.
(27) Berreman, D. W.; Meiboom, S. Tensor representation of Oseen-Frank strain energy in uniaxial cholesterics. *Phys. Rev. A: At., Mol., Opt. Phys.* **1984**, *30*, 1955−1959.
(28) Longa, L.; Monselesan, D.; Trebin, H.-R. An extension of the Landau-Ginzburg-de Gennes theory for liquid crystals. *Liq. Cryst.* **1987**, *2*, 769−796.
(29) Longa, L. On the tricritical point of the nematic−smectic A phase transition in liquid crystals. *J. Chem. Phys.* **1986**, *85*, 2974.
(30) Longa, L.; Trebin, H.-R. Structure of the elastic free energy for chiral nematic liquid crystals. *Phys. Rev. A: At., Mol., Opt. Phys.* **1989**, *39*, 2160−2168.
(31) Longa, L.; Tomczyk, W. Twist-bend nematic phase in the presence of molecular chirality. *Liq. Cryst.* **2018**, *45*, 2074−2085.
(32) Allender, D.; Longa, L. Landau-de Gennes theory of biaxial nematics reexamined. *Phys. Rev. E: Stat., Nonlinear, Soft Matter Phys.* **2008**, *78*, 011704−011714.
(33) Greco, C.; Ferrarini, A. Entropy-driven chiral order in a system of achiral bent particles. *Phys. Rev. Lett.* **2015**, *115*, 147801−147805.
(34) Gramsbergen, E. F.; Longa, L.; de Jeu, W. H. Landau theory of the nematic-isotropic phase transition. *Phys. Rep.* **1986**, *135*, 195−257.
(35) Longa, L.; Pająk, G. 2016; See Supplemental Material of [*Phys. Rev. E: Stat., Nonlinear, Soft Matter Phys.* **2016**, *93*, 040701(R)], which is available at: http://journals.aps.org/pre/supplemental/10.1103/PhysRevE.93.040701/Supplemental_material.pdf.
(36) Greco, C.; Luckhurst, G. R.; Ferrarini, A. Molecular geometry, twist-bend nematic phase and unconventional elasticity: a generalised Maier-Saupe theory. *Soft Matter* **2014**, *10*, 9318−9323.
(37) Ferrarini, A. The twist-bend nematic phase: Molecular insights from a generalised Maier-Saupe theory. *Liq. Cryst.* **2017**, *44*, 45−57.
(38) Osipov, M. A.; Pająk, G. Effect of polar intermolecular interactions on the elastic constants of bent-core nematics and the origin of the twist-bend phase. *Eur. Phys. J. E* **2016**, *39*, 45−56.

https://dx.doi.org/10.1021/acs.jpcc.0c05711
J. Phys. Chem. C 2020, 124, 22761−22775

(39) Tomczyk, W.; Pająk, G.; Longa, L. Twist-bend nematic phases of bent-shaped biaxial molecules. *Soft Matter* **2016**, *12*, 7445−7452.
(40) Tomczyk, W.; Longa, L. Role of molecular bend angle and biaxiality in the stabilization of the twist-bend nematic phase. *Soft Matter* **2020**, *16*, 4350−4357.
(41) Kats, E. I.; Lebedev, V. V.; Muratov, A. R. Weak crystallization theory. *Phys. Rep.* **1993**, *228*, 1−91.
(42) López, D. O.; Sebastian, N.; de la Fuente, M. R.; Martínez-García, J. C.; Salud, J.; Pérez-Jubindo, M. A.; Diez-Berart, S.; Dunmur, D. A.; Luckhurst, G. R. Disentangling molecular motions involved in the glass transition of a twist-bend nematic liquid crystal through dielectric studies. *J. Chem. Phys.* **2012**, *137*, 034502−034511.
(43) Paterson, D. A.; Abberley, J. P.; Harrison, W. T. A.; Storey, J. M. D.; Imrie, C. T. Cyanobiphenyl-based liquid crystal dimers and the twist-bend nematic phase. *Liq. Cryst.* **2017**, *44*, 127−146.
(44) Zhu, C.; Tuchband, M. R.; Young, A.; Shuai, M.; Scarbrough, A.; Walba, D. M.; Maclennan, J. E.; Wang, C.; Hexemer, A.; Clark, N. A. Resonant carbon *K*-edge soft X-ray scattering from lattice-free heliconical molecular ordering: soft dilative elasticity of the twist-bend liquid crystal phase. *Phys. Rev. Lett.* **2016**, *116*, 147803−147808.
(45) Meyer, C.; Luckhurst, G. R.; Dozov, I. The temperature dependence of the heliconical tilt angle in the twist-bend nematic phase of the odd dimer CB7CB. *J. Mater. Chem. C* **2015**, *3*, 318−328.
(46) Tuchband, M. R.; Shuai, M.; Graber, K. A.; Chen, D.; Zhu, C.; Radzihovsky, L.; Klittnick, A.; Foley, L. M.; Scarbrough, A.; Porada, J. H. et al. Double-helical tiled chain structure of the twist-bend liquid crystal phase in CB7CB. **2017**, arXiv:1703.10787
(47) Jokisaari, J. P.; Luckhurst, G. R.; Timimi, B. A.; Zhu, J.; Zimmermann, H. Twist-bend nematic phase of the liquid crystal dimer CB7CB: orientational order and conical angle determined by ^{129}Xe and ^{2}H NMR spectroscopy. *Liq. Cryst.* **2015**, *42*, 708−721.
(48) Vaupotič, N.; Ali, M.; Majewski, P. W.; Gorecka, E.; Pociecha, D. Polarization gratings spontaneously formed from a helical twist-bend nematic phase. *ChemPhysChem* **2018**, *19*, 2566−2571.
(49) Mandle, R. J.; Goodby, J. W. Order parameters, orientational distribution functions and heliconical tilt angles of oligomeric liquid crystals. *Phys. Chem. Chem. Phys.* **2019**, *21*, 6839−6843.
(50) Singh, G.; Fu, J.; Agra-Kooijman, D. M.; Song, J.-K.; Vengatesan, M. R.; Srinivasarao, M.; Fisch, M. R.; Kumar, S. X-ray and Raman scattering study of orientational order in nematic and heliconical nematic liquid crystals. *Phys. Rev. E: Stat., Nonlinear, Soft Matter Phys.* **2016**, *94*, 060701−060706.
(51) Zhang, Z.; Panov, V. P.; Nagaraj, M.; Mandle, R. J.; Goodby, J. W.; Luckhurst, G. R.; Jones, J. C.; Gleeson, H. F. Raman scattering studies of order parameters in liquid crystalline dimers exhibiting the nematic and twist-bend nematic phases. *J. Mater. Chem. C* **2015**, *3*, 10007−10016.
(52) Salamończyk, M.; Vaupotič, N.; Pociecha, D.; Wang, C.; Zhu, C.; Gorecka, E. 2017; See Supplemental Material of [*Soft Matter* **2017**, *13*, 6694], which is available at: www.rsc.org/suppdata/c7/sm/c7sm00967d/c7sm00967d1.pdf.
(53) Salamończyk, M.; Vaupotič, N.; Pociecha, D.; Wang, C.; Zhu, C.; Gorecka, E. Structure of nanoscale-pitch helical phases: blue phase and twist-bend nematic phase resolved by resonant soft X-ray scattering. *Soft Matter* **2017**, *13*, 6694−6699.
(54) Salamończyk, M.; Mandle, R. J.; Makal, A.; Liebman-Peláez, A.; Feng, J.; Goodby, J. W.; Zhu, C. Double helical structure of the twist-bend nematic phase investigated by resonant X-ray scattering at the carbon and sulfur K-edges. *Soft Matter* **2018**, *14*, 9760−9763.
(55) Stevenson, W. D.; Ahmed, Z.; Zeng, X. B.; Welch, C.; Ungar, G.; Mehl, G. H. Molecular organization in the twist-bend nematic phase by resonant X-ray scattering at the Se K-edge and by SAXS, WAXS and GIXRD. *Phys. Chem. Chem. Phys.* **2017**, *19*, 13449−13454.
(56) Madhusudana, N. V.; Pratibha, R. Elasticity and Orientational Order in Some Cyanobiphenyls: Part IV. Reanalysis of the Data. *Mol. Cryst. Liq. Cryst.* **1982**, *89*, 249−257.
(57) Delaye, M.; Ribotta, R.; Durand, G. Rayleigh Scattering at a Second-Order Nematic to Smectic-*A* Phase Transition. *Phys. Rev. Lett.* **1973**, *31*, 443−445.
(58) Blinc, R.; Muševič, I. In *Handbook of Liquid Crystals Set*; Demus, D., Goodby, J., Gray, G. W., Spiess, H. W., Vill, V., Eds.; John Wiley & Sons, Ltd, 1998; Chapter 2.6, pp 170−197.
(59) Shi, J.; Sidky, H.; Whitmer, J. K. Novel elastic response in twist-bend nematic models. *Soft Matter* **2019**, *15*, 8219−8226.
(60) Čopič, M.; Mertelj, A. Q-tensor model of twist-bend and splay nematic phases. *Phys. Rev. E: Stat., Nonlinear, Soft Matter Phys.* **2020**, *101*, 022704−022709.
(61) Anzivino, C.; van Roij, R.; Dijkstra, M. A Landau-de Gennes theory for twist-bend and splay-bend nematic phases of colloidal suspensions of bent rods. *J. Chem. Phys.* **2020**, *152*, 224502−224514.

https://dx.doi.org/10.1021/acs.jpcc.0c05711
J. Phys. Chem. C 2020, 124, 22761−22775

Supporting Information for

"Twist-Bend Nematic Phase from Landau-de Gennes Perspective"

Lech Longa* and Wojciech Tomczyk†

Institute of Theoretical Physics, Jagiellonian University, Łojasiewicza 11, 30–348 Kraków, Poland

I. ELASTIC FREE ENERGY OF NEMATIC LIQUID CRYSTALS

The expansion of the free energy in powers of $\tilde{Q}_{\alpha\beta}$ and its derivatives up to the order $\tilde{\mathbf{Q}}\,\tilde{\mathbf{Q}}\,\partial\tilde{\mathbf{Q}}\,\partial\tilde{\mathbf{Q}}$ contains twenty-two terms. They are [1]:

$\partial\tilde{\mathbf{Q}}\,\partial\tilde{\mathbf{Q}}$:

$$\begin{aligned}
\left[L_1^{(2)}\right] &= \tilde{Q}_{\alpha\beta,\,\gamma}\,\tilde{Q}_{\alpha\beta,\,\gamma},\\
\left[L_2^{(2)}\right] &= \tilde{Q}_{\alpha\beta,\,\beta}\,\tilde{Q}_{\alpha\gamma,\,\gamma},\\
\left[L_3^{(2)}\right] &= \tilde{Q}_{\alpha\beta,\,\gamma}\,\tilde{Q}_{\alpha\gamma,\,\beta}.
\end{aligned} \tag{S.1}$$

$\tilde{\mathbf{Q}}\,\partial\tilde{\mathbf{Q}}\,\partial\tilde{\mathbf{Q}}$:

$$\begin{aligned}
\left[L_1^{(3)}\right] &= \tilde{Q}_{\alpha\beta}\,\tilde{Q}_{\alpha\beta,\,\mu}\,\tilde{Q}_{\mu\nu,\,\nu}, & \left[L_2^{(3)}\right] &= \tilde{Q}_{\alpha\beta}\,\tilde{Q}_{\alpha\mu,\,\beta}\,\tilde{Q}_{\mu\nu,\,\nu},\\
\left[L_3^{(3)}\right] &= \tilde{Q}_{\alpha\beta}\,\tilde{Q}_{\alpha\mu,\,\mu}\,\tilde{Q}_{\beta\nu,\,\nu}, & \left[L_4^{(3)}\right] &= \tilde{Q}_{\alpha\beta}\,\tilde{Q}_{\alpha\mu,\,\nu}\,\tilde{Q}_{\beta\mu,\,\nu},\\
\left[L_5^{(3)}\right] &= \tilde{Q}_{\alpha\beta}\,\tilde{Q}_{\alpha\mu,\,\nu}\,\tilde{Q}_{\beta\nu,\,\mu}, & \left[L_6^{(3)}\right] &= \tilde{Q}_{\alpha\beta}\,\tilde{Q}_{\alpha\mu,\,\nu}\,\tilde{Q}_{\mu\nu,\,\beta}.
\end{aligned} \tag{S.2}$$

$\tilde{\mathbf{Q}}\,\tilde{\mathbf{Q}}\,\partial\tilde{\mathbf{Q}}\,\partial\tilde{\mathbf{Q}}$:

$$\begin{aligned}
\left[L_1^{(4)}\right] &= \left(\mathrm{Tr}\,\tilde{\mathbf{Q}}^2\right)\tilde{Q}_{\varrho\mu,\,\varrho}\,\tilde{Q}_{\mu\nu,\,\nu}, & \left[L_2^{(4)}\right] &= \left(\mathrm{Tr}\,\tilde{\mathbf{Q}}^2\right)\tilde{Q}_{\mu\nu,\,\varrho}\,\tilde{Q}_{\mu\nu,\,\varrho},\\
\left[L_3^{(4)}\right] &= \left(\mathrm{Tr}\,\tilde{\mathbf{Q}}^2\right)\tilde{Q}_{\mu\nu,\,\varrho}\,\tilde{Q}_{\varrho\mu,\,\nu}, & \left[L_4^{(4)}\right] &= \tilde{Q}_{\alpha\varrho}\,\tilde{Q}_{\varrho\beta}\,\tilde{Q}_{\alpha\beta,\,\mu}\,\tilde{Q}_{\mu\nu,\,\nu},\\
\left[L_5^{(4)}\right] &= \tilde{Q}_{\alpha\varrho}\,\tilde{Q}_{\varrho\beta}\,\tilde{Q}_{\alpha\mu,\,\beta}\,\tilde{Q}_{\mu\nu,\,\nu}, & \left[L_6^{(4)}\right] &= \tilde{Q}_{\alpha\varrho}\,\tilde{Q}_{\varrho\beta}\,\tilde{Q}_{\alpha\mu,\,\mu}\,\tilde{Q}_{\beta\nu,\,\nu},\\
\left[L_7^{(4)}\right] &= \tilde{Q}_{\alpha\varrho}\,\tilde{Q}_{\beta\varrho}\,\tilde{Q}_{\alpha\mu,\,\nu}\,\tilde{Q}_{\beta\mu,\,\nu}, & \left[L_8^{(4)}\right] &= \tilde{Q}_{\alpha\varrho}\,\tilde{Q}_{\varrho\beta}\,\tilde{Q}_{\alpha\mu,\,\nu}\,\tilde{Q}_{\beta\nu,\,\mu},\\
\left[L_9^{(4)}\right] &= \tilde{Q}_{\alpha\varrho}\,\tilde{Q}_{\varrho\beta}\,\tilde{Q}_{\alpha\mu,\,\nu}\,\tilde{Q}_{\mu\nu,\,\beta}, & \left[L_{10}^{(4)}\right] &= \tilde{Q}_{\alpha\beta}\,\tilde{Q}_{\mu\varrho}\,\tilde{Q}_{\beta\mu,\,\alpha}\,\tilde{Q}_{\varrho\nu,\,\nu},\\
\left[L_{11}^{(4)}\right] &= \tilde{Q}_{\alpha\beta}\,\tilde{Q}_{\mu\varrho}\,\tilde{Q}_{\mu\nu,\,\alpha}\,\tilde{Q}_{\varrho\nu,\,\beta}, & \left[L_{12}^{(4)}\right] &= \tilde{Q}_{\alpha\beta}\,\tilde{Q}_{\mu\varrho}\,\tilde{Q}_{\alpha\beta,\,\nu}\,\tilde{Q}_{\nu\varrho,\,\mu},\\
\left[L_{13}^{(4)}\right] &= \tilde{Q}_{\alpha\beta}\,\tilde{Q}_{\mu\varrho}\,\tilde{Q}_{\alpha\beta,\,\nu}\,\tilde{Q}_{\mu\varrho,\,\nu}.
\end{aligned} \tag{S.3}$$

* E–mail address: lech.longa@uj.edu.pl

† E–mail address: wojciech.tomczyk@doctoral.uj.edu.pl

In defining stability conditions we will also use the $\left[L_{14}^{(4)}\right]$ invariant, which is a linear combination of $\left[L_{1}^{(4)}\right]\ldots\left[L_{13}^{(4)}\right]$:

$$\left[L_{14}^{(4)}\right] \equiv \tilde{Q}_{\alpha\beta}\tilde{Q}_{\gamma\delta}\tilde{Q}_{\alpha\mu,\beta}\tilde{Q}_{\gamma\mu,\delta} = -\frac{\left[L_{1}^{(4)}\right]}{2} + \frac{\left[L_{2}^{(4)}\right]}{2}\left[L_{3}^{(4)}\right] - 2\left[L_{4}^{(4)}\right] + \left[L_{6}^{(4)}\right] - \left[L_{7}^{(4)}\right] + \left[L_{8}^{(4)}\right] + 2\left[L_{9}^{(4)}\right] + \left[L_{11}^{(4)}\right] \quad \text{(S.4)}$$

II. EFFECTIVE ELASTIC CONSTANTS

The effective elastic constants $K_{ii}^{(n)}$ for $i = 1, 2, 3$ and $n = 2, 3, 4$ expressed in terms of $\left[L_{m}^{(n)}\right]$, Equation (S.1-S.4). Included in decomposition is also $\left[L_{14}^{(4)}\right]$:

For $n = 2$:

$$\begin{aligned} K_{11}^{(2)} &= 2\left(2L_{1}^{(2)} + L_{2}^{(2)} + L_{3}^{(2)}\right), \\ K_{22}^{(2)} &= 4L_{1}^{(2)}, \\ K_{33}^{(2)} &= 2\left(2L_{1}^{(2)} + L_{2}^{(2)} + L_{3}^{(2)}\right). \end{aligned} \quad \text{(S.5)}$$

For $n = 3$:

$$\begin{aligned} K_{11}^{(3)} &= \frac{2}{3}\left(-L_{2}^{(3)} + 2L_{3}^{(3)} + L_{4}^{(3)} + 2L_{5}^{(3)} - L_{6}^{(3)}\right), \\ K_{22}^{(3)} &= \frac{2}{3}L_{4}^{(3)}, \\ K_{33}^{(3)} &= \frac{2}{3}\left(2L_{2}^{(3)} - L_{3}^{(3)} + L_{4}^{(3)} - L_{5}^{(3)} + 2L_{6}^{(3)}\right). \end{aligned} \quad \text{(S.6)}$$

For $n = 4$:

$$\begin{aligned} K_{11}^{(4)} &= \frac{2}{9}\left(6L_{1}^{(4)} + 12L_{2}^{(4)} + 6L_{3}^{(4)} + L_{5}^{(4)} + 4L_{6}^{(4)} + 5L_{7}^{(4)} + 4L_{8}^{(4)} + L_{9}^{(4)} - 2L_{10}^{(4)} - L_{11}^{(4)} + L_{14}^{(4)}\right), \\ K_{22}^{(4)} &= \frac{2}{9}\left(12L_{2}^{(4)} + 5L_{7}^{(4)} - L_{11}^{(4)}\right), \\ K_{33}^{(4)} &= \frac{2}{9}\left(6L_{1}^{(4)} + 12L_{2}^{(4)} + 6L_{3}^{(4)} + 4L_{5}^{(4)} + L_{6}^{(4)} + 5L_{7}^{(4)} + L_{8}^{(4)} + 4L_{9}^{(4)} - 2L_{10}^{(4)} + 2L_{11}^{(4)} + 4L_{14}^{(4)}\right). \end{aligned} \quad \text{(S.7)}$$

III. A COMPLETE EXPRESSION FOR FREE ENERGY DENSITY OF UNIFORMLY DEFORMED STRUCTURES (UDSs)

$$
\begin{aligned}
f_{Qb} &= t_Q \left(r_1^2 + r_2^2 + x_0^2\right) - \frac{x_0 \left(x_0^2 - 3\, r_2^2\right)}{\sqrt{6}} - \frac{1}{4} r_1^2 \left(3\sqrt{2}\, r_2 \cos\left(2\,\chi_1 - \chi_2\right) + \sqrt{6}\, x_0\right) \\
&+ c_b \left(r_1^2 + r_2^2 + x_0^2\right)^2 \\
&+ d_b \left(r_1^2 + r_2^2 + x_0^2\right) \left(\frac{1}{4} r_1^2 \left(3\sqrt{2}\, r_2 \cos\left(2\,\chi_1 - \chi_2\right) + \sqrt{6}\, x_0\right) + \frac{x_0 \left(x_0^2 - 3\, r_2^2\right)}{\sqrt{6}}\right) \\
&+ \left(\frac{1}{4} r_1^2 \left(3\sqrt{2}\, r_2 \cos\left(2\,\chi_1 - \chi_2\right) + \sqrt{6}\, x_0\right) + \frac{x_0 \left(x_0^2 - 3 r_2^2\right)}{\sqrt{6}}\right)^2 \qquad \text{(S.8)} \\
&+ e_b \left(\left(r_1^2 + r_2^2 + x_0^2\right)^3 - \frac{1}{12} \left(3 r_1^2 (3\cos(2\,\chi_1 - \chi_2) r_2 + \sqrt{3} x_0) + 2\sqrt{3} x_0 (-3 r_2^2 + x_0^2)\right)^2\right), \\
f_{Qel} &= \frac{1}{12} k^2 \left[24\, \rho_{4,7}\, r_2^4 + r_2^2 \left(48\, \kappa_1 + 3\left(9\, \rho_{4,7} + 8\, \rho_{4,15}\right) r_1^2 - 8\sqrt{6}\, \rho_{3,4} x_0 + 8\, \rho_{4,7}\, x_0^2\right)\right. \\
&+ r_1^2 \left(6\, \kappa_2 + 3\, \rho_{4,7}\, r_1^2 + \sqrt{6}\left(\rho_{3,4} - 4\, \rho_{3,7}\right) x_0 + \left(5\, \rho_{4,7} + 8\, \rho_{4,15}\right) x_0^2\right) \\
&+ \left. r_1^2\, r_2 \left(9\sqrt{2}\, \rho_{3,4} - 12\sqrt{2}\, \rho_{3,7} + 2\sqrt{3}\left(3\, \rho_{4,7} + 8\, \rho_{4,15}\right) x_0\right) \cos\left(2\,\chi_1 - \chi_2\right)\right], \qquad \text{(S.9)}
\end{aligned}
$$

$$
f_P = t_P \left(p_1^2 + v_0^2\right) + k^2 p_1^2 + a_d \left(p_1^2 + v_0^2\right)^2, \qquad \text{(S.10)}
$$

$$
f_{QP} = \frac{k\, p_1 r_1 e_P \sin\left(\chi_1\right)}{\sqrt{2}} - \frac{\lambda\, p_1^2\, r_2 \cos\left(\chi_2\right)}{\sqrt{2}} - \sqrt{2}\, \lambda\, p_1 r_1 v_0 \cos\left(\chi_1\right) + \frac{\lambda\, p_1^2 x_0}{\sqrt{6}} - \sqrt{\frac{2}{3}} \lambda\, v_0^2 x_0. \qquad \text{(S.11)}
$$

IV. EXPERIMENTAL DATA AND NUMERICAL RESULTS

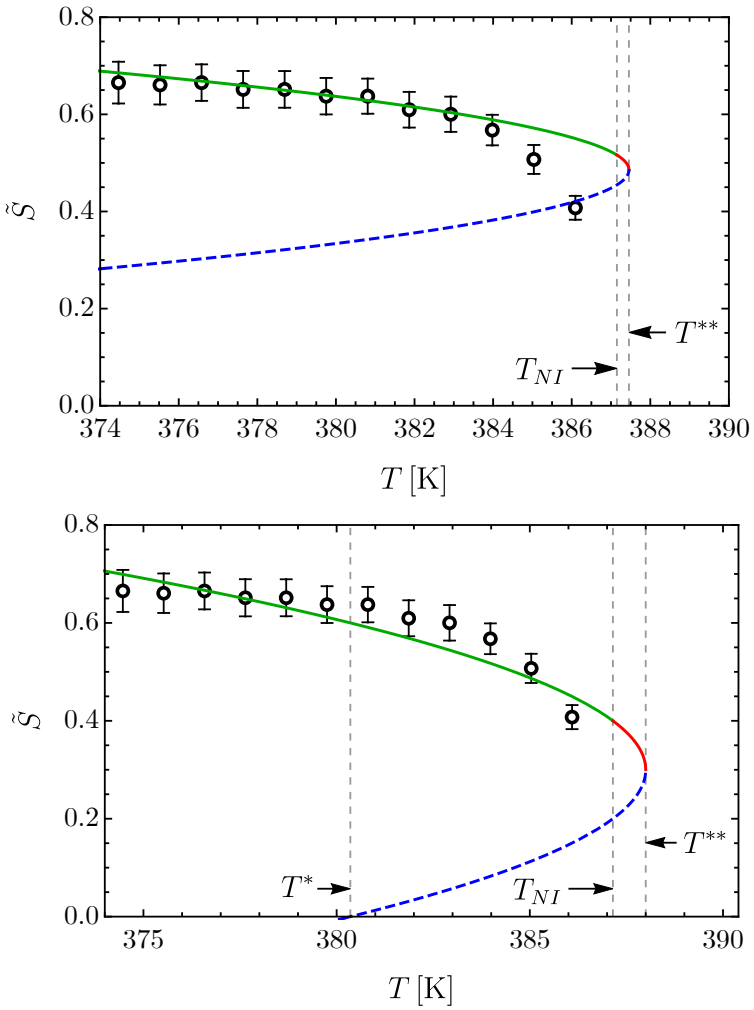

Figure S1. Exemplary results for fitting $\tilde{S}$ predicted by fourth order bulk free energy of LdeG expansion to experimental data. Please observe a large discrepancy between predicted and measured $T_{NI} - T^*$ difference. As can be seen the smallest value of $T_{NI} - T^*$ obtained from fitting the data for CB7CB is $T_{NI} - T^* \gtrsim 7\,\mathrm{K}$, while experimentally $T_{NI} - T^* < 1\,\mathrm{K}$.

Table S1. Basic experimental data for CB7CB used for estimating some of the parameters of the extended LdeG theory, along with other crucial data resulting from the aforementioned approach.

Nematic

Description	Parameter	Value	Unit	Source
Temperature of nematic-isotropic phase transition	T_{NI}	387.15	K	Ref. [2]
Supercooling temperature of the isotropic phase	T^*	386	K	acquired from $\tilde{S}(T)$
Enthalpy of nematic-isotropic phase transition	ΔH_{NI}	0.72	kJ/mol	Ref. [3]
Order parameter at T_{NI}	$\tilde{S}_{NI}$	0.3	-	acquired from $\tilde{S}(T = T_{NI})$

Twist-bend nematic

Description	Parameter	Value	Unit	Source
Temperature of twist-bend nematic to nematic phase transition	$T_{N_{\mathrm{TB}}N}$	374.15	K	Ref. [2]
Enthalpy of twist-bend nematic to nematic phase transition	$\Delta H_{N_{\mathrm{TB}}N}$	0.83	kJ/mol	Ref. [3]

Table S2. Values of fitted coefficients of the bulk (38) and elastic constants (42) expansions, along with ones resulting from the flexopolarization renormalization. Additionally, according to (14) and (43) $K_{ii}^{(n)}$ elastic constants are provided.

Coefficient	Value $\left[\times 10^7\,\mathrm{J/m^3}\right]$	Coefficient	Value [pN]	Coefficient	Value [pN]
a_{0Q}	2.66	$K_{11}^{(2)} = K_{33}^{(2)}$	9.85	$L_1^{(2)}$	0.93
b	0.27	$K_{22}^{(2)}$	4.23	$L_2^{(2)}$	-0.0045
c	0.60	$K_{11}^{(3)}$	11.08	$L_2^{(3)}$	-11.16
d	-3.80	$K_{22}^{(3)}$	0.60	$L_3^{(3)}$	2.27
f	9.64	$K_{33}^{(3)}$	-15.80	$L_4^{(3)}$	0.90
		$K_{11}^{(4)}$	9.93	$L_6^{(4)}$	6.29
		$K_{22}^{(4)}$	1.77	$L_7^{(4)}$	1.59
		$K_{33}^{(4)}$	13.45	$L_{14}^{(4)}$	11.56
				$\frac{\varepsilon_P^2}{4a_P}$	0.08
				$\frac{\Lambda_{\mathrm{QP}}\varepsilon_P^2}{4a_P^2}$	0.00013
$T_P = 362$ K					

Table S3. Dimensionless parameters related to bulk part, elastic constants and bifurcation equations. Below are provided converters for $\Delta t \leftrightarrow t_Q$, $\tilde{\mathbf{r}} \leftrightarrow \mathbf{r}$ and $\tilde{\mathbf{k}} \leftrightarrow \mathbf{k}$.

Parameter	Value	Parameter	Value	Parameter	Value
c_b	0.67	$\rho_{2,2}$	-0.0048	l_2	-1.58
d_b	-1.29	$\rho_{3,2}$	-3.64	l_3	0.59
Δt_{NI}	0.0029	$\rho_{3,3}$	0.74	l_4	0.93
		$\rho_{3,4}$	0.29	κ_1	1.13
		$\rho_{4,6}$	0.62	κ_2	5.38
		$\rho_{4,7}$	0.15	κ_3	-7.73
		$\rho_{4,14}$	1.14	κ_4	6.0054

$$t_Q = 32.36(\Delta t + \Delta t_{NI}) \qquad \tilde{\mathbf{r}}\,[\mathrm{nm}] = 1.06\,\mathbf{r} \qquad \tilde{\mathbf{k}}\,[\mathrm{nm}^{-1}] = 0.94\,\mathbf{k}$$

Table S4. Temperature ranges in Δt and t_Q units for stable liquid crystalline structures: nematic and twist-bend nematic from experiment [2].

Range of temperature parameter	Description
$-0.03 < \Delta t \leq 0$	nematic
$\Delta t \leq -0.03$	twist-bend nematic
$-0.99 < t_Q \leq 0.09$	nematic
$t_Q \leq -0.99$	twist-bend nematic

[1] Longa, L.; Monselesan, D.; Trebin, H.-R. An extension of the Landau-Ginzburg-de Gennes theory for liquid crystals. *Liq. Cryst.* **1987**, *2*, 769–796.

[2] Babakhanova, G.; Parsouzi, Z.; Paladugu, S.; Wang, H.; Nastishin, Y. A.; Shiyanovskii, S. V.; Sprunt, S.; Lavrentovich, O. D. Elastic and viscous properties of the nematic dimer CB7CB. *Phys. Rev. E* **2017**, *96*, 062704–062715.

[3] Paterson, D. A.; Abberley, J. P.; Harrison, W. T. A.; Storey, J. M. D.; Imrie, C. T. Cyanobiphenyl-based liquid crystal dimers and the twist-bend nematic phase. *Liq. Cryst.* **2017**, *44*, 127–146.